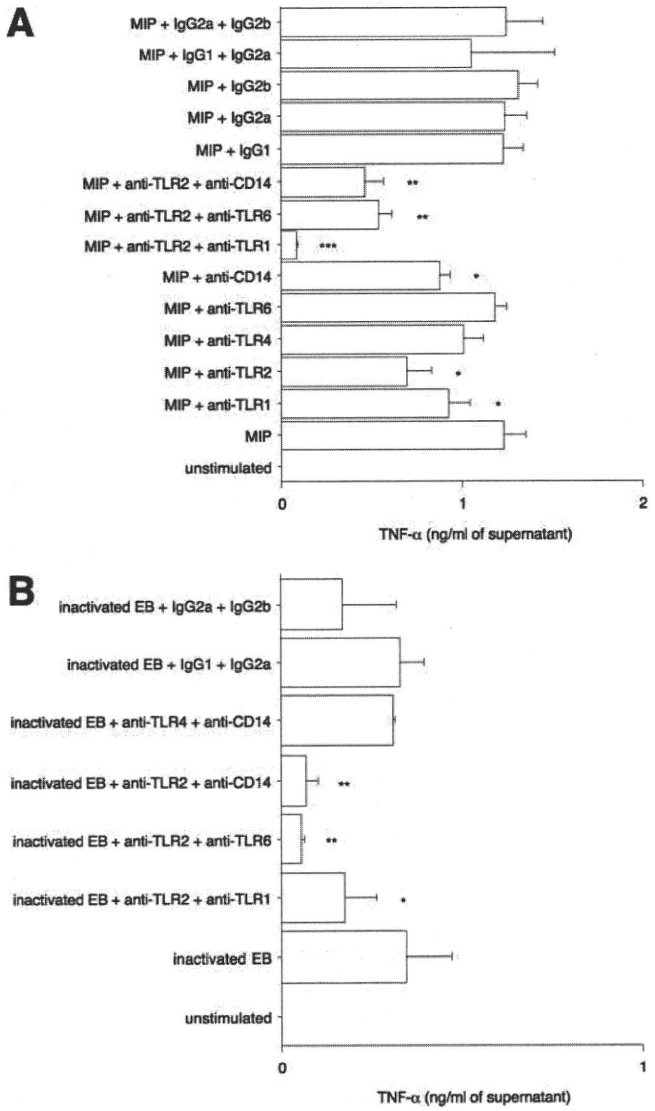

FIGURE 11. The production of TNF-α by PMA-differentiated THP-1 cells upon rMip or inactivated *C. trachomatis* EB activation is mainly TLR2/TLR1/TLR6/CD14 dependent. PMA-differentiated THP-1 cells were preincubated for 1 h with 50 μg/ml human IgG to block Fc receptors and prevent nonspecific binding of blocking Ab or control IgG. Cells were next preincubated for 1 h at 37°C in the presence or absence of 5 μg/ml of various blocking mAbs: anti-TLR1, anti-TLR2, anti-TLR4, anti-TLR6, anti-CD14, or isotype-matched mouse IgG1, IgG2a, and IgG2b controls alone or associated before addition of either 1 μg/ml rMip (*A*) or inactivated *C. trachomatis* EB (5×10^6/ml) (*B*). Results were expressed as TNF-α concentrations obtained in each condition, included pretreatment of cells with isotype controls. Each value represents mean ± SD of triplicates from one representative of two or three independent experiments with similar results. *, $p < 0.05$; **, $p < 0.005$; ***, $p < 0.0001$ determined by comparison with control using Student's *t* test.

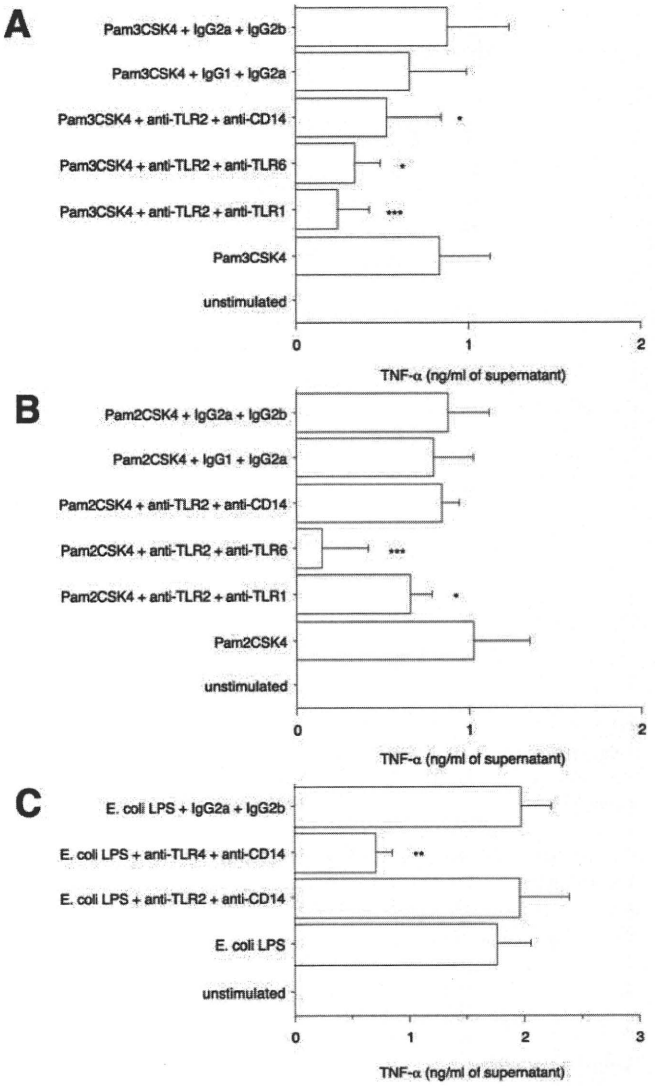

FIGURE 12. Host receptors involved in activation of THP-1 cells by control lipopeptides and *E. coli* LPS. PMA-differentiated THP-1 cells were preincubated for 1 h with 50 μg/ml human IgG to block Fc receptors and prevent nonspecific binding of blocking Ab or control IgG. Cells were next preincubated for 1 h at 37°C in the presence or absence of 5 μg/ml of various association of blocking mAbs: anti-TLR1/TLR2, anti-TLR2/TLR6, anti-TLR2/CD14, anti-TLR4/CD14, or isotype-matched mouse IgG before addition of 0.01 μg/ml lipopeptides (Pam_3CSK_4 (*A*) or Pam_2CSK_4 (*B*)) or 1 μg/ml *E. coli* LPS (*C*). Results were expressed as TNF-α concentrations obtained in each condition, included pretreatment of cells with isotype controls. Each value represents mean ± SD of triplicates from one representative of two or three independent experiments with similar results. *, $p < 0.05$; **, $p < 0.005$; ***, $p < 0.0001$ were determined by comparison with control using Student's *t* test.

of anti-TLR2 with anti-CD14, anti-TLR1, or anti-TLR6 led to significant inhibitions ($p < 0.05$ to 0.0001) of TNF-α secretion, the association of anti-TLR2 with anti-TLR1 being the most inhibitory, as shown in Fig. 12*A*. When Pam_2CSK_4 was used as stimulant, the pretreatment of THP-1 cells with the combination of anti-TLR2 with anti-TLR1 or anti-TLR6 led to significant inhibitions ($p < 0.05$ to 0.0001) of TNF-α secretion, the association of anti-TLR2 with anti-TLR6 being the most inhibitory, as shown in Fig. 12*B*. These data show no clear-cut segregation of Pam_3CSK_4 and Pam_2CSK_4 interactions with TLR2/TLR1 or TLR2/TLR6 (62–65) but rather a tendency of Pam_3CSK_4 to stimulate THP-1 cells more efficiently via TLR2/TLR1 and Pam_2CSK_4 via TLR2/TLR6. Because *E. coli* LPS is commonly used as TLR4 and CD14-ligand (66), it was also used as control and tested in the same conditions. The pretreatment of THP-1 cells with the combination of anti-TLR4 with anti-CD14 led to significant inhibitions of TNF-α secretion ($p < 0.005$), whereas no inhibition was obtained with the combination of anti-TLR2 with anti-CD14, as shown in Fig. 12*C*. In all these experiments, no significant change of cytokine production was induced by nonimmune mouse IgG used as controls instead of each mAb.

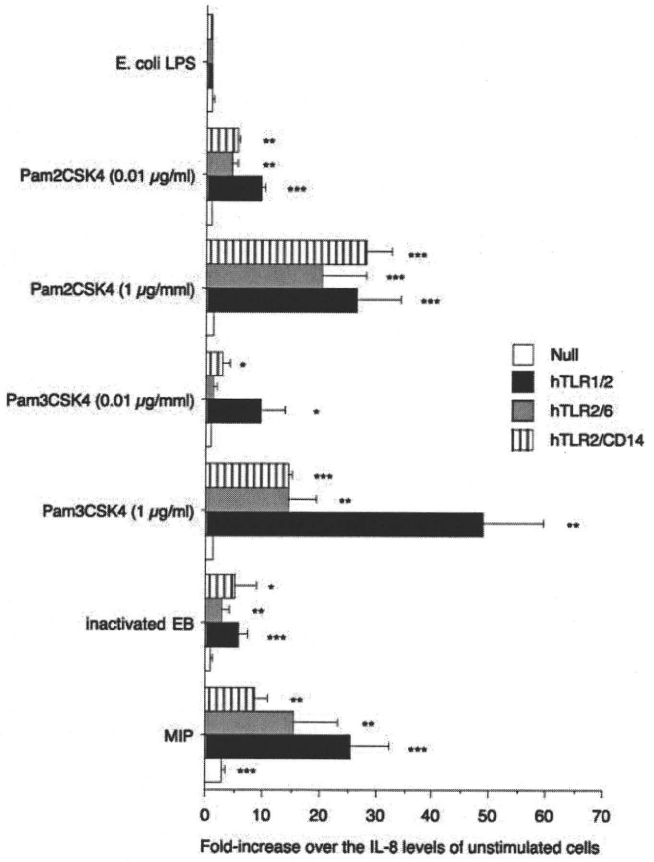

FIGURE 13. The production of IL-8 by HEK-293 cell lines expressing human TLR1/2, TLR2/6, or TLR2/CD14 upon rMip or inactivated *C. trachomatis* EB activation is mainly TLR2/TLR1/TLR6/CD14 dependent. Null, hTLR1/2, hTLR2/6, and hTLR2/CD14 cells were stimulated with 1 μg/ml rMip, inactivated *C. trachomatis* EB (5×10^6/ml), 1 or 0.01 μg/ml lipopeptides (Pam_3CSK_4 or Pam_2CSK_4), or 1 μg/ml *E. coli* LPS for 24 h. Culture supernatants were collected, and IL-8 content was analyzed. The results are expressed in terms of fold increase over the IL-8 levels of unstimulated cells. Each value represents mean ± SD of triplicates from three independent experiments. *, $p < 0.05$; **, $p < 0.005$; ***, $p < 0.0001$ determined by one sample *t* test; mean is significantly different from 1.

CD14, TLR1, TLR2, and TLR6 are involved in rMip activation of HEK-293 cell lines expressing human TLR1/2, TLR2/6, or TLR2/CD14

To further ensure proper identification of receptors involved in the recognition of rMip and to assess their respective contribution, a cell model using HEK-293 cells transfected with human TLR1/2, TLR2/6, or TLR2/CD14 genes was used. Null cells lacking TLRs and CD14 responded to rMip by producing a 2.8-fold increase of IL-8 release in absence of stimulation, indicating that rMip was able to slightly stimulate these cells in absence of TLRs and CD14 but no response was observed with other stimulants. In contrast, HEK-293 cells expressing either hTLR1/2, or hTLR2/6, or hTLR2/CD14 responded to all stimulants, except *E. coli* LPS. The highest stimulatory effect of rMip was obtained under the condition of hTLR1/2 coexpression that led to a 26-fold higher release of IL-8 than in absence of stimulant ($p < 0.0001$). The hTLR2/6 and hTLR2/CD14 coexpressions led to a 16- and 9-fold increase of IL-8 release ($p < 0.005$), respectively. In presence of inactivated *C. trachomatis* EB, the highest stimulatory effect was also obtained under the condition of hTLR1/2 coexpression that led to a 6-fold higher release of IL-8 than in absence of stimulant ($p < 0.0001$). The hTLR2/6 and hTLR2/CD14 coexpressions led to a 3- and 5-fold increase of IL-8 release ($p < 0.05$ to 0.005), respectively. These results agree with those obtained in blocking experiments. In presence of lipopeptides, the effects were dependent upon the stimulating concentrations. At 1 μg/ml concentration, HEK-293 cells coexpressing hTLR1/2, hTLR2/6, or hTLR2/CD14 responded to both Pam_3CSK_4 and Pam_2CSK_4. The highest stimulatory effect of Pam_3CSK_4 was obtained under the condition of hTLR1/2 coexpression that led to a 49-fold increase whereas the coexpression of hTLR2/6 led to a 15-fold increase of IL-8 release ($p < 0.005$). When hTLR1/2 genes were coexpressed, Pam_2CSK_4 stimulation led to a lower increase of IL-8 release than under Pam_3CSK_4 stimulation (26- vs 49-fold) but when hTLR2/6 genes were coexpressed, Pam_2CSK_4 stimulation led only to a slightly higher increase of IL-8 release than under Pam_3CSK_4 stimulation (20 vs 15-fold). In contrast, when the stimulating concentration was 0.01 μg/ml, Pam_3CSK_4 was still able to stimulate HEK-293 cells coexpressing hTLR1/2 that led to a 11-fold increase of IL-8 release ($p < 0.05$) but was no more able to stimulate cells coexpressing hTLR2/6. However, Pam_2CSK_4 was still able to stimulate HEK-293 cells coexpressing hTLR1/2 and coexpressing hTLR2/6 that led to a 9- and 5-fold increase of IL-8 release, respectively ($p < 0.005$), as shown in Fig. 13. These results agree with those obtained in blocking experiments except that blocking of both TLR2 and TLR6 slightly inhibited Pam_3CSK_4 activation and that blocking of both TLR2 and CD14 did not inhibit Pam_2CSK activation. These discrepancies could be explained by different expression ratios of TLR6 and CD14 in HEK compared with THP-1 cells. Taken together, these data indicate that rMip, inactivated *C. trachomatis* EB, Pam_3CSK_4, and Pam_2CSK_4 are only partially TLR1-, TLR6-, and CD14-dependent. These results are therefore partially contradictory to previous reports identifying TLR1 as the sole coreceptor for triacylated lipopeptides (62), and TLR6 as the sole coreceptor for diacylated lipopeptides (67) while supporting results of other groups (68–70).

Discussion

The present study demonstrates that among seven individual chlamydial components, rMip was the most effective to induce a proinflammatory cytokine response in human monocytes/macrophages (peripheral blood monocytes and THP-1 cell line). Even if rMip responses were lower than those induced by *E. coli* and *S. typhimurium* LPS, they were significant in contrast to *Chlamydia* LPS, as already reported (10, 15, 36, 71). IL-8 was the dominant cytokine induced by rMip in vitro and this observation must be related to the cytokine patterns present in vivo during infection by chlamydiae where high levels of IL-8 were reported in tears from children with trachoma, as well as in endocervical secretions obtained from women infected with *Chlamydia* (72).

The proinflammatory activity induced by WT rMip was not due to *E. coli* LPS contamination, as determined by the *Limulus* Amoebocyte lysate assay, insensitivity to polymyxin B, different serum requirement, and absence of inhibition by anti-TLR4 Abs. The stimulatory activities of WT rMip were similar to those of native Mip and appeared to be dependent upon lipid modification because nonlipidated C20A rMip variant was devoid of effect on cytokine release. In addition, WT rMip activity was greatly reduced by alkaline hydrolysis or treatment with lipases but was unaffected by heat or proteinase K treatments. The cell receptors involved in rMip and *C. trachomatis* EB cellular activation were determined using two independent assays that clearly demonstrated the involvement of TLR1/2/6 and CD14 but not TLR4. The main receptors involved in rMip activation were TLR1/2 but the co-presence of TLR1, TLR6, and CD14 was not absolutely required

because activation was possible by TLR1/2, TLR2/6, or TLR2/CD14. In these assays, the receptors involved in Pam_3CSK_4 and Pam_2CSK_4 activation did not completely agree with the original concept, according to which triacylated lipopeptides recognize TLR2/TLR1 heteromers, whereas diacylated lipopeptides recognize TLR2/TLR6 heteromers (63, 65, 73) but agree with other reports (68–70). Indeed, the ability of Pam_3CSK_4 to stimulate HEK-293 cells coexpressing hTLR1/2 and, to a lesser extent, hTLR2/6 has been reported (68) and Pam_3CSK_4 has been shown to exhibit some activity toward TLR2/6 when used at high concentrations (69). Pam_2CSK_4 has been shown to exhibit comparable activities toward both the human TLR2/1 and TLR2/6 pairs (69) and macrophages of TLR6-deficient mice to be fully responsive to Pam_2CSK_4 (70). In fact the number of acyl-residues, the peptide sequence and the whole molecular structure of the lipopeptide/lipoprotein have been shown to be responsible for TLR2/1- or TLR2/6-dependent signaling (70, 74). The involvement of CD14 in rMip activation agrees with other studies showing that bacterial lipoproteins (53, 56, 57, 75, 76), Pam_3CSK_4 (53, 77), and Pam_2CSK_4 (68) interact with CD14 to cause cytokine induction. These results agree with reports showing a predominant role of TLR2 in *C. trachomatis* (78) as well as *C. pneumoniae* recognition (14, 19, 79) and with results of Netea et al. (14) attributing proinflammatory cytokine production to non-LPS components. The fact that rMip and EB act through the same receptors and that anti-rMip Ab is able to partly inhibit EB-mediated TNF-α release suggest a role of native Mip, present at the EB surface (20), or other surface lipoproteins in EB recognition and macrophage activation in natural infection. If IL-1β, TNF-α, and IL-6 release in response to native Mip or other lipoproteins may aid in eradicating *Chlamydia* infection (80–83), particularly if their levels increase early (83), these cytokines may also promote long-term tissue damage. As an example, high levels of TNF-α have been associated with detrimental effects in ocular chlamydial infection (84). Moreover, Mip-induced IL-8 can be deleterious (83), particularly in case of chronic secretion. Indeed, IL-8 promotes the infiltration of neutrophils that are not only inefficient in resolving chlamydial infections but can release proteases that damage cells. In addition and as reported for other bacterium-associated lipoproteins (85), Mip or other lipoproteins could be released from EB surface (either from living bacteria or from bacteria lysed as a result of effective host defense or the activities of certain antibiotics) and retained inside tissues where they might activate resident cells and perpetuate inflammation even after the eradication of live bacteria with antibiotic therapy. Lipoproteins are considered as crucial virulence factors in inflammatory processes and in pathogenesis of several important bacterial infections, such as those triggered by *Mycobacterium tuberculosis* (76), *Neisseria gonorrhoeae* (86), *Listeria monocytogenes* (58, 87), *Brucella abortus* (88), and members of Enterobacteriaceae family (89, 90). In organisms such as *Borrelia burgdorferi* and *Treponema pallidum*, which lack LPS, bacterial lipoproteins are known to play an important role in pathogenesis (49, 75, 88, 91–93). In chlamydiae, LPS is a major structural component of all chlamydial species (22) but compared with the LPS of enterobacteria, it has much lower endotoxin activity (10, 71, 94, 95) because its lipid A is highly hydrophobic and has unique structural features with the presence of unusual, long-chain fatty acids (96). *Chlamydia* LPS is unable to elicit inflammation in experimental animals (13) and is a weak inducer of the inflammatory cytokine response (10, 36, 37), as shown in the present study. All these data support the hypothesis that in chlamydiae, Mip or other lipoproteins might play a key role in pathogenesis. The fact that Mip is present in the membrane of EBs as well as reticulate bodies (97) and was recently shown to be surface exposed by two different approaches (20) reinforces its potential role in pathogenesis of *Chlamydia* infection. If the exact chemical nature of *Chlamydia*-derived monocyte/macrophage stimulators is not known, the fact that receptors involved in Mip recognition are similar to those involved in *C. trachomatis* EB recognition is supportive of the involvement of Mip or other *Chlamydia*-associated lipoproteins as inflammatory active element of EB.

In conclusion, this study is the first report about a chlamydial lipoprotein displaying proinflammatory properties. As Mip appears to be present in different species of the Chlamydiaceae family (20), it could have an important role in the inflammatory aspects of trachoma, reactive arthritis, or atherogenesis.

Acknowledgment

We thank Yvette Froment for technical support.

Disclosures

The authors have no financial conflict of interest.

References

1. Hahn, D. L., R. W. Dodge, and R. Golubjatnikov. 1991. Association of *Chlamydia pneumoniae* (strain TWAR) infection with wheezing, asthmatic bronchitis, and adult-onset asthma. *J. Am. Med. Assoc.* 266: 225–230.
2. Centers for Disease Control and Prevention. 1997. *Chlamydia trachomatis* genital infections–United States, 1995. *J. Am. Med. Assoc.* 277: 952–953.
3. Kalayoglu, M. V., P. Libby, and G. I. Byrne. 2002. *Chlamydia pneumoniae* as an emerging risk factor in cardiovascular disease. *J. Am. Med. Assoc.* 288: 2724–2731.
4. Mabey, D. C., A. W. Solomon, and A. Foster. 2003. Trachoma. *Lancet* 362: 223–229.
5. Corsaro, D., and G. Greub. 2006. Pathogenic potential of novel Chlamydiae and diagnostic approaches to infections due to these obligate intracellular bacteria. *Clin. Microbiol. Rev.* 19: 283–297.
6. Patton, D. L., and C. C. Kuo. 1989. Histopathology of *Chlamydia trachomatis* salpingitis after primary and repeated reinfections in the monkey subcutaneous pocket model. *J. Reprod Fertil.* 85: 647–656.
7. Kiviat, N. B., J. A. Paavonen, P. Wolner-Hanssen, C. W. Critchlow, W. E. Stamm, J. Douglas, D. A. Eschenbach, L. A. Corey, and K. K. Holmes. 1990. Histopathology of endocervical infection caused by *Chlamydia trachomatis*, herpes simplex virus, Trichomonas vaginalis, and *Neisseria gonorrhoeae*. *Hum. Pathol.* 21: 831–837.
8. Morrison, R. P., R. J. Belland, K. Lyng, and H. D. Caldwell. 1989. Chlamydial disease pathogenesis. The 57-kD chlamydial hypersensitivity antigen is a stress response protein. *J. Exp. Med.* 170: 1271–1283.
9. Rothermel, C. D., J. Schachter, P. Lavrich, E. C. Lipsitz, and T. Francus. 1989. *Chlamydia trachomatis*-induced production of interleukin-1 by human monocytes. *Infect. Immun.* 57: 2705–2711.
10. Ingalls, R. R., P. A. Rice, N. Qureshi, K. Takayama, J. S. Lin, and D. T. Golenbock. 1995. The inflammatory cytokine response to *Chlamydia trachomatis* infection is endotoxin mediated. *Infect. Immun.* 63: 3125–3130.
11. Kol, A., G. K. Sukhova, A. H. Lichtman, and P. Libby. 1998. Chlamydial heat shock protein 60 localizes in human atheroma and regulates macrophage tumor necrosis factor-α and matrix metalloproteinase expression. *Circulation* 98: 300–307.
12. Kol, A., T. Bourcier, A. H. Lichtman, and P. Libby. 1999. Chlamydial and human heat shock protein 60s activate human vascular endothelium, smooth muscle cells, and macrophages. *J. Clin. Invest.* 103: 571–577.
13. Watkins, N. G., W. J. Hadlow, A. B. Moos, and H. D. Caldwell. 1986. Ocular delayed hypersensitivity: a pathogenetic mechanism of chlamydial-conjunctivitis in guinea pigs. *Proc. Natl. Acad. Sci. USA* 83: 7480–7484.
14. Netea, M. G., B. J. Kullberg, J. M. Galama, A. F. Stalenhoef, C. A. Dinarello, and J. W. Van der Meer. 2002. Non-LPS components of *Chlamydia pneumoniae* stimulate cytokine production through Toll-like receptor 2-dependent pathways. *Eur. J. Immunol.* 32: 1188–1195.
15. Prebeck, S., H. Brade, C. J. Kirschning, C. P. da Costa, S. Durr, H. Wagner, and T. Miethke. 2003. The Gram-negative bacterium *Chlamydia trachomatis* L2 stimulates tumor necrosis factor secretion by innate immune cells independently of its endotoxin. *Microbes Infect.* 5: 463–470.
16. Vabulas, R. M., P. Ahmad-Nejad, C. da Costa, T. Miethke, C. J. Kirschning, H. Hacker, and H. Wagner. 2001. Endocytosed HSP60s use toll-like receptor 2 (TLR2) and TLR4 to activate the toll/interleukin-1 receptor signaling pathway in innate immune cells. *J. Biol. Chem.* 276: 31332–31339.
17. Sasu, S., D. LaVerda, N. Qureshi, D. T. Golenbock, and D. Beasley. 2001. *Chlamydia pneumoniae* and chlamydial heat shock protein 60 stimulate proliferation of human vascular smooth muscle cells via toll-like receptor 4 and p44/p42 mitogen-activated protein kinase activation. *Circ. Res.* 89: 244–250.
18. Bulut, Y., E. Faure, L. Thomas, H. Karahashi, K. S. Michelsen, O. Equils, S. G. Morrison, R. P. Morrison, and M. Arditi. 2002. Chlamydial heat shock protein 60 activates macrophages and endothelial cells through Toll-like receptor 4 and MD2 in a MyD88-dependent pathway. *J. Immunol.* 168: 1435–1440.

19. Prebeck, S., C. Kirschning, S. Durr, C. da Costa, B. Donath, K. Brand, V. Redecke, H. Wagner, and T. Miethke. 2001. Predominant role of toll-like receptor 2 versus 4 in *Chlamydia pneumoniae*-induced activation of dendritic cells. *J. Immunol.* 167: 3316–3323.
20. Neff, L., S. Daher, P. Muzzin, U. Spenato, F. Gülacar, C. Gabay, and S. Bas. 2007. Molecular characterization and subcellular localization of macrophage infectivity potentiator, a *Chlamydia trachomatis* lipoprotein. *J. Bacteriol.* 189: 4739–4748.
21. Boleti, H., A. Benmerah, D. M. Ojcius, N. Cerf-Bensussan, and A. Dautry-Varsat. 1999. Chlamydia infection of epithelial cells expressing dynamin and Eps15 mutants: clathrin-independent entry into cells and dynamin-dependent productive growth. *J. Cell Sci.* 112(Pt. 10): 1487–1496.
22. Rund, S., B. Lindner, H. Brade, and O. Holst. 1999. Structural analysis of the lipopolysaccharide from *Chlamydia trachomatis* serotype L2. *J. Biol. Chem.* 274: 16819–16824.
23. Hirschfeld, M., Y. Ma, J. H. Weis, S. N. Vogel, and J. J. Weis. 2000. Cutting edge: repurification of lipopolysaccharide eliminates signaling through both human and murine toll-like receptor 2. *J. Immunol.* 165: 618–622.
24. Bas, S., P. Muzzin, B. Ninet, J. E. Bornand, C. Scieux, and T. L. Vischer. 2001. Chlamydial serology: comparative diagnostic value of immunoblotting, microimmunofluorescence test, and immunoassays using different recombinant proteins as antigens. *J. Clin. Microbiol.* 39: 1368–1377.
25. Bas, S., P. Muzzin, and T. L. Vischer. 2001. *Chlamydia trachomatis* serology: diagnostic value of outer membrane protein 2 compared with that of other antigens. *J. Clin. Microbiol.* 39: 4082–4085.
26. Bausinger, H., D. Lipsker, U. Ziylan, S. Manié, J. P. Briand, J. P. Cazenave, S. Muller, J. F. Haeuw, C. Ravanat, H. de la Salle, and D. Hanau. 2002. Endotoxin-free heat-shock protein 70 fails to induce APC activation. *Eur. J. Immunol.* 32: 3708–3713.
27. Gao, B., and M. F. Tsan. 2003. Recombinant human heat shock protein 60 does not induce the release of tumor necrosis factor α from murine macrophages. *J. Biol. Chem.* 278: 22523–22529.
28. Gao, B., and M. F. Tsan. 2003. Endotoxin contamination in recombinant human heat shock protein 70 (Hsp70) preparation is responsible for the induction of tumor necrosis factor α release by murine macrophages. *J. Biol. Chem.* 278: 174–179.
29. Nakao, Y., K. Funami, S. Kikkawa, M. Taniguchi, M. Nishiguchi, Y. Fukumori, T. Seya, and M. Matsumoto. 2005. Surface-expressed TLR6 participates in the recognition of diacylated lipopeptide and peptidoglycan in human cells. *J. Immunol.* 174: 1566–1573.
30. Armant, M., M. Rubio, G. Delespesse, and M. Sarfati. 1995. Soluble CD23 directly activates monocytes to contribute to the antigen-independent stimulation of resting T cells. *J. Immunol.* 155: 4868–4875.
31. Burger, D., N. Molnarfi, L. Gruaz, and J. M. Dayer. 2004. Differential induction of IL-1β and TNF by CD40 ligand or cellular contact with stimulated T cells depends on the maturation stage of human monocytes. *J. Immunol.* 173: 1292–1297.
32. Tsuchiya, S., M. Yamabe, Y. Yamaguchi, Y. Kobayashi, T. Konno, and K. Tada. 1980. Establishment and characterization of a human acute monocytic leukemia cell line (THP-1). *Int. J. Cancer* 26: 171–176.
33. Muhlradt, P. F., and M. Frisch. 1994. Purification and partial biochemical characterization of a *Mycoplasma fermentans*-derived substance that activates macrophages to release nitric oxide, tumor necrosis factor, and interleukin-6. *Infect. Immun.* 62: 3801–3807.
34. Pleiss, J., M. Fischer, and R. D. Schmid. 1998. Anatomy of lipase binding sites: the scissile fatty acid binding site. *Chem. Phys. Lipids* 93: 67–80.
35. Vidal, V., I. G. Scragg, S. J. Cutler, K. A. Rockett, D. Fekade, D. A. Warrell, D. J. Wright, and D. Kwiatkowski. 1998. Variable major lipoprotein is a principal TNF-inducing factor of louse-borne relapsing fever. *Nat. Med.* 4: 1416–1420.
36. Brade, L., S. Schramek, U. Schade, and H. Brade. 1986. Chemical, biological, and immunochemical properties of the *Chlamydia psittaci* lipopolysaccharide. *Infect. Immun.* 54: 568–574.
37. Karimi, S. T., R. H. Schloemer, and C. E. Wilde, III. 1989. Accumulation of chlamydial lipopolysaccharide antigen in the plasma membranes of infected cells. *Infect. Immun.* 57: 1780–1785.
38. Häupl, T., S. Landgraf, P. Netusil, N. Biller, C. Capiau, P. Desmons, P. Hauser, and G. R. Burmester. 1997. Activation of monocytes by three OspA vaccine candidates: lipoprotein OspA is a potent stimulator of monokines. *FEMS Immunol. Med. Microbiol.* 19: 15–23.
39. Murthy, P. K., V. A. Dennis, B. L. Lasater, and M. T. Philipp. 2000. Interleukin-10 modulates proinflammatory cytokines in the human monocytic cell line THP-1 stimulated with *Borrelia burgdorferi* lipoproteins. *Infect. Immun.* 68: 6663–6669.
40. Auwerx, J. 1991. The human leukemia cell line, THP-1: a multifacetted model for the study of monocyte-macrophage differentiation. *Experientia* 47: 22–31.
41. Schumann, R. R., S. R. Leong, G. W. Flaggs, P. W. Gray, S. D. Wright, J. C. Mathison, P. S. Tobias, and R. J. Ulevitch. 1990. Structure and function of lipopolysaccharide binding protein. *Science* 249: 1429–1431.
42. Wright, S. D., R. A. Ramos, P. S. Tobias, R. J. Ulevitch, and J. C. Mathison. 1990. CD14, a receptor for complexes of lipopolysaccharide (LPS) and LPS binding protein. *Science* 249: 1431–1433.
43. Corradin, S. B., J. Mauel, P. Gallay, D. Heumann, R. J. Ulevitch, and P. S. Tobias. 1992. Enhancement of murine macrophage binding of and response to bacterial lipopolysaccharide (LPS) by LPS-binding protein. *J. Leukocyte Biol.* 52: 363–368.
44. Hailman, E., H. S. Lichenstein, M. M. Wurfel, D. S. Miller, D. A. Johnson, M. Kelley, L. A. Busse, M. M. Zukowski, and S. D. Wright. 1994. Lipopolysaccharide (LPS)-binding protein accelerates the binding of LPS to CD14. *J. Exp. Med.* 179: 269–277.
45. Lundemose, A. G., D. A. Rouch, S. Birkelund, G. Christiansen, and J. H. Pearce. 1992. *Chlamydia trachomatis* Mip-like protein. *Mol. Microbiol.* 6: 2539–2548.
46. Muhlradt, P. F., H. Meyer, and R. Jansen. 1996. Identification of *S*-(2,3-dihydroxypropyl)cystein in a macrophage-activating lipopeptide from *Mycoplasma fermentans*. *Biochemistry* 35: 7781–7786.
47. Brandt, M. E., B. S. Riley, J. D. Radolf, and M. V. Norgard. 1990. Immunogenic integral membrane proteins of *Borrelia burgdorferi* are lipoproteins. *Infect. Immun.* 58: 983–991.
48. Shimizu, T., Y. Iwamoto, Y. Yanagihara, M. Kurimura, and K. Achiwa. 1994. Mitogenic activity and the induction of tumor necrosis factor by lipopeptide analogs of the N-terminal part of lipoprotein in the outer membrane of *Escherichia coli*. *Biol. Pharm. Bull.* 17: 980–982.
49. Radolf, J. D., L. L. Arndt, D. R. Akins, L. L. Curetty, M. E. Levi, Y. Shen, L. S. Davis, and M. V. Norgard. 1995. *Treponema pallidum* and *Borrelia burgdorferi* lipoproteins and synthetic lipopeptides activate monocytes/macrophages. *J. Immunol.* 154: 2866–2877.
50. Metzger, J. W., A. G. Beck-Sickinger, M. Loleit, M. Eckert, W. G. Bessler, and G. Jung. 1995. Synthetic *S*-(2,3-dihydroxypropyl)-cysteinyl peptides derived from the N-terminus of the cytochrome subunit of the photoreaction centre of *Rhodopseudomonas viridis* enhance murine splenocyte proliferation. *J. Pept. Sci.* 1: 184–190.
51. Muhlradt, P. F., M. Kiess, H. Meyer, R. Sussmuth, and G. Jung. 1997. Isolation, structure elucidation, and synthesis of a macrophage stimulatory lipopeptide from *Mycoplasma fermentans* acting at picomolar concentration. *J. Exp. Med.* 185: 1951–1958.
52. Janeway, C. A., Jr., and R. Medzhitov. 2002. Innate immune recognition. *Annu. Rev. Immunol.* 20: 197–216.
53. Sellati, T. J., D. A. Bouis, R. L. Kitchens, R. P. Darveau, J. Pugin, R. J. Ulevitch, S. C. Gangloff, S. M. Goyert, M. V. Norgard, and J. D. Radolf. 1998. *Treponema pallidum* and *Borrelia burgdorferi* lipoproteins and synthetic lipopeptides activate monocytic cells via a CD14-dependent pathway distinct from that used by lipopolysaccharide. *J. Immunol.* 160: 5455–5464.
54. Visintin, A., A. Mazzoni, J. H. Spitzer, D. H. Wyllie, S. K. Dower, and D. M. Segal. 2001. Regulation of Toll-like receptors in human monocytes and dendritic cells. *J. Immunol.* 166: 249–255.
55. Triantafilou, M., K. Triantafilou, and N. Fernandez. 2000. Rough and smooth forms of fluorescein-labelled bacterial endotoxin exhibit CD14/LBP dependent and independent binding that is influenced by endotoxin concentration. *Eur. J. Biochem.* 267: 2218–2226.
56. Wooten, R. M., T. B. Morrison, J. H. Weis, S. D. Wright, R. Thieringer, and J. J. Weis. 1998. The role of CD14 in signaling mediated by outer membrane lipoproteins of *Borrelia burgdorferi*. *J. Immunol.* 160: 5485–5492.
57. Giambartolomei, G. H., V. A. Dennis, B. L. Lasater, and M. T. Philipp. 1999. Induction of pro- and anti-inflammatory cytokines by *Borrelia burgdorferi* lipoproteins in monocytes is mediated by CD14. *Infect. Immun.* 67: 140–147.
58. Flo, T. H., O. Halaas, E. Lien, L. Ryan, G. Teti, D. T. Golenbock, A. Sundan, and T. Espevik. 2000. Human toll-like receptor 2 mediates monocyte activation by *Listeria monocytogenes*, but not by group B streptococci or lipopolysaccharide. *J. Immunol.* 164: 2064–2069.
59. Wyllie, D. H., E. Kiss-Toth, A. Visintin, S. C. Smith, S. Boussouf, D. M. Segal, G. W. Duff, and S. K. Dower. 2000. Evidence for an accessory protein function for Toll-like receptor 1 in anti-bacterial responses. *J. Immunol.* 165: 7125–7132.
60. Shimazu, R., S. Akashi, H. Ogata, Y. Nagai, K. Fukudome, K. Miyake, and M. Kimoto. 1999. MD-2, a molecule that confers lipopolysaccharide responsiveness on Toll-like receptor 4. *J. Exp. Med.* 189: 1777–1782.
61. Akashi, S., H. Ogata, F. Kirikae, T. Kirikae, K. Kawasaki, M. Nishijima, R. Shimazu, Y. Nagai, K. Fukudome, M. Kimoto, and K. Miyake. 2000. Regulatory roles for CD14 and phosphatidylinositol in the signaling via toll-like receptor 4-MD-2. *Biochem. Biophys. Res. Commun.* 268: 172–177.
62. Takeuchi, O., S. Sato, T. Horiuchi, K. Hoshino, K. Takeda, Z. Dong, R. L. Modlin, and S. Akira. 2002. Cutting edge: role of Toll-like receptor 1 in mediating immune response to microbial lipoproteins. *J. Immunol.* 169: 10–14.
63. Akira, S. 2003. Mammalian Toll-like receptors. *Curr. Opin. Immunol.* 15: 5–11.
64. Sandor, F., E. Latz, F. Re, L. Mandell, G. Repik, D. T. Golenbock, T. Espevik, E. A. Kurt-Jones, and R. W. Finberg. 2003. Importance of extra- and intracellular domains of TLR1 and TLR2 in NFκB signaling. *J. Cell Biol.* 162: 1099–1110.
65. Takeuchi, O., T. Kawai, P. F. Muhlradt, M. Morr, J. D. Radolf, A. Zychlinsky, K. Takeda, and S. Akira. 2001. Discrimination of bacterial lipoproteins by Toll-like receptor 6. *Int. Immunol.* 13: 933–940.
66. Takeda, K., T. Kaisho, and S. Akira. 2003. Toll-like receptors. *Annu. Rev. Immunol.* 21: 335–376.
67. Morr, M., O. Takeuchi, S. Akira, M. M. Simon, and P. F. Muhlradt. 2002. Differential recognition of structural details of bacterial lipopeptides by toll-like receptors. *Eur. J. Immunol.* 32: 3337–3347.
68. Schroder, N. W., H. Heine, C. Alexander, M. Manukyan, J. Eckert, L. Hamann, U. B. Gobel, and R. R. Schumann. 2004. Lipopolysaccharide binding protein binds to triacylated and diacylated lipopeptides and mediates innate immune responses. *J. Immunol.* 173: 2683–2691.
69. Omueti, K. O., J. M. Beyer, C. M. Johnson, E. A. Lyle, and R. I. Tapping. 2005. Domain exchange between human toll-like receptors 1 and 6 reveals a region required for lipopeptide discrimination. *J. Biol. Chem.* 280: 36616–36625.
70. Buwitt-Beckmann, U., H. Heine, K. H. Wiesmuller, G. Jung, R. Brock, S. Akira, and A. J. Ulmer. 2005. Toll-like receptor 6-independent signaling by diacylated lipopeptides. *Eur. J. Immunol.* 35: 282–289.

71. Heine, H., S. Müller-Loennies, L. Brade, B. Lindner, and H. Brade. 2003. Endotoxic activity and chemical structure of lipopolysaccharides from *Chlamydia trachomatis* serotypes E and L2 and *Chlamydophila psittaci* 6BC. *Eur. J. Biochem.* 270: 440–450.
72. Stephens, R. S. 2003. The cellular paradigm of chlamydial pathogenesis. *Trends Microbiol.* 11: 44–51.
73. Takeda, K., O. Takeuchi, and S. Akira. 2002. Recognition of lipopeptides by Toll-like receptors. *J. Endotoxin Res.* 8: 459–463.
74. Okusawa, T., M. Fujita, J. Nakamura, T. Into, M. Yasuda, A. Yoshimura, Y. Hara, A. Hasebe, D. T. Golenbock, M. Morita, et al. 2004. Relationship between structures and biological activities of mycoplasmal diacylated lipopeptides and their recognition by toll-like receptors 2 and 6. *Infect. Immun.* 72: 1657–1665.
75. Hirschfeld, M., C. J. Kirschning, R. Schwandner, H. Wesche, J. H. Weis, R. M. Wooten, and J. J. Weis. 1999. Cutting edge: inflammatory signaling by *Borrelia burgdorferi* lipoproteins is mediated by toll-like receptor 2. *J. Immunol.* 163: 2382–2386.
76. Brightbill, H. D., D. H. Libraty, S. R. Krutzik, R. B. Yang, J. T. Belisle, J. R. Bleharski, M. Maitland, M. V. Norgard, S. E. Plevy, S. T. Smale, et al. 1999. Host defense mechanisms triggered by microbial lipoproteins through toll-like receptors. *Science* 285: 732–736.
77. Manukyan, M., K. Triantafilou, M. Triantafilou, A. Mackie, N. Nilsen, T. Espevik, K. H. Wiesmuller, A. J. Ulmer, and H. Heine. 2005. Binding of lipopeptide to CD14 induces physical proximity of CD14, TLR2 and TLR1. *Eur. J. Immunol.* 35: 911–921.
78. Darville, T., J. M. O'Neill, C. W. Andrews, Jr., U. M. Nagarajan, L. Stahl, and D. M. Ojcius. 2003. Toll-like receptor-2, but not Toll-like receptor-4, is essential for development of oviduct pathology in chlamydial genital tract infection. *J. Immunol.* 171: 6187–6197.
79. Netea, M. G., J. W. van der Meer, M. van Deuren, and B. J. Kullberg. 2003. Proinflammatory cytokines and sepsis syndrome: not enough, or too much of a good thing? *Trends Immunol.* 24: 254–258.
80. Williams, D. M., D. M. Magee, L. F. Bonewald, J. G. Smith, C. A. Bleicker, G. I. Byrne, and J. Schachter. 1990. A role in vivo for tumor necrosis factor α in host defense against *Chlamydia trachomatis*. *Infect. Immun.* 58: 1572–1576.
81. Darville, T., C. W. Andrews, Jr., K. K. Laffoon, W. Shymasani, L. R. Kishen, and R. G. Rank. 1997. Mouse strain-dependent variation in the course and outcome of chlamydial genital tract infection is associated with differences in host response. *Infect. Immun.* 65: 3065–3073.
82. Williams, D. M., B. G. Grubbs, T. Darville, K. Kelly, and R. G. Rank. 1998. A role for interleukin-6 in host defense against murine *Chlamydia trachomatis* infection. *Infect. Immun.* 66: 4564–4567.
83. Darville, T., C. W. Andrews, Jr., J. D. Sikes, P. L. Fraley, and R. G. Rank. 2001. Early local cytokine profiles in strains of mice with different outcomes from chlamydial genital tract infection. *Infect. Immun.* 69: 3556–3561.
84. Conway, D. J., M. J. Holland, R. L. Bailey, A. E. Campbell, O. S. Mahdi, R. Jennings, E. Mbena, and D. C. Mabey. 1997. Scarring trachoma is associated with polymorphism in the tumor necrosis factor α (TNF-α) gene promoter and with elevated TNF-α levels in tear fluid. *Infect. Immun.* 65: 1003–1006.
85. Hellman, J., P. M. Loiselle, M. M. Tehan, J. E. Allaire, L. A. Boyle, J. T. Kurnick, D. M. Andrews, K. Sik Kim, and H. S. Warren. 2000. Outer membrane protein A, peptidoglycan-associated lipoprotein, and murein lipoprotein are released by *Escherichia coli* bacteria into serum. *Infect. Immun.* 68: 2566–2572.
86. Fisette, P. L., S. Ram, J. M. Andersen, W. Guo, and R. R. Ingalls. 2003. The Lip lipoprotein from *Neisseria gonorrhoeae* stimulates cytokine release and NF-κB activation in epithelial cells in a Toll-like receptor 2-dependent manner. *J. Biol. Chem.* 278: 46252–46260.
87. Réglier-Poupet, H., C. Frehel, I. Dubail, J. L. Beretti, P. Berche, A. Charbit, and C. Raynaud. 2003. Maturation of lipoproteins by type II signal peptidase is required for phagosomal escape of *Listeria monocytogenes*. *J. Biol. Chem.* 278: 49469–49477.
88. Giambartolomei, G. H., A. Zwerdling, J. Cassataro, L. Bruno, C. A. Fossati, and M. T. Philipp. 2004. Lipoproteins, not lipopolysaccharide, are the key mediators of the proinflammatory response elicited by heat-killed *Brucella abortus*. *J. Immunol.* 173: 4635–4642.
89. Zhang, H., J. W. Peterson, D. W. Niesel, and G. R. Klimpel. 1997. Bacterial lipoprotein and lipopolysaccharide act synergistically to induce lethal shock and proinflammatory cytokine production. *J. Immunol.* 159: 4868–4878.
90. Hellman, J., J. D. Roberts, Jr., M. M. Tehan, J. E. Allaire, and H. S. Warren. 2002. Bacterial peptidoglycan-associated lipoprotein is released into the bloodstream in Gram-negative sepsis and causes inflammation and death in mice. *J. Biol. Chem.* 277: 14274–14280.
91. Infante-Duarte, C., and T. Kamradt. 1997. Lipopeptides of *Borrelia burgdorferi* outer surface proteins induce Th1 phenotype development in alphabeta T-cell receptor transgenic mice. *Infect. Immun.* 65: 4094–4099.
92. Porcella, S. F., and T. G. Schwan. 2001. *Borrelia burgdorferi* and *Treponema pallidum*: a comparison of functional genomics, environmental adaptations, and pathogenic mechanisms. *J. Clin. Invest.* 107: 651–656.
93. Thoma-Uszynski, S., S. Stenger, O. Takeuchi, M. T. Ochoa, M. Engele, P. A. Sieling, P. F. Barnes, M. Rollinghoff, P. L. Bolcskei, M. Wagner, et al. 2001. Induction of direct antimicrobial activity through mammalian toll-like receptors. *Science* 291: 1544–1547.
94. Nurminen, M., M. Leinonen, P. Saikku, and P. H. Makela. 1983. The genus-specific antigen of *Chlamydia*: resemblance to the lipopolysaccharide of enteric bacteria. *Science* 220: 1279–1281.
95. Brade, H., L. Brade, and F. E. Nano. 1987. Chemical and serological investigations on the genus-specific lipopolysaccharide epitope of *Chlamydia*. *Proc. Natl. Acad. Sci. USA* 84: 2508–2512.
96. Kosma, P. 1999. Chlamydial lipopolysaccharide. *Biochim. Biophys. Acta* 1455: 387–402.
97. Lundemose, A. G., S. Birkelund, S. J. Fey, P. M. Larsen, and G. Christiansen. 1991. *Chlamydia trachomatis* contains a protein similar to the *Legionella pneumophila mip* gene product. *Mol. Microbiol.* 5: 109–115.

Tumor-Secreted Lactic Acid Promotes IL-23/IL-17 Proinflammatory Pathway[1]

Hiroaki Shime,* Masahiko Yabu,* Takashi Akazawa,* Ken Kodama,† Misako Matsumoto,‡ Tsukasa Seya,‡ and Norimitsu Inoue[2]*

IL-23 is a proinflammatory cytokine consisting of a p19 subunit and a p40 subunit that is shared with IL-12. IL-23 is overexpressed in and around tumor tissues, where it induces local inflammation and promotes tumor development. Many tumor cells produce large amounts of lactic acid by altering their glucose metabolism. In this study, we show that lactic acid secreted by tumor cells enhances the transcription of *IL-23p19* and IL-23 production in monocytes/macrophages and in tumor-infiltrating immune cells that are stimulated with TLR2 and 4 ligands. DNA elements responsible for this enhancing activity of lactic acid were detected in a 2.7-kb 5′-flanking region of the human *IL-23p19* gene. The effect of lactic acid was strictly regulated by extracellular pH. Furthermore, by inducing IL-23 overproduction, lactic acid facilitated the Ag-dependent secretion of proinflammatory cytokine IL-17 but not IFN-γ by TLR ligand-stimulated mouse splenocytes. Interestingly, this effect was observed even in the absence of TLR ligand stimulation. These results suggest that rather than just being a terminal metabolite, lactic acid is a proinflammatory mediator that is secreted by tumor cells to activate the IL-23/IL-17 proinflammatory pathway but not the Th1 pathway. Targeting the lactic acid-induced proinflammatory response may be a useful approach for treating cancer. *The Journal of Immunology,* 2008, 180: 7175–7183.

Immune cells often infiltrate in and around many kinds of tumors. Initially, the immune system protects the host from cancer development and, indeed, the infiltration of NK cells in cancers is associated with a favorable prognosis (1). However, the infiltration of innate-immune cells such as macrophages correlates with a poor prognosis, which suggests that these cells may be directly involved in tumor development and metastasis by inducing angiogenesis and tissue remodeling. Moreover, many cancers often arise at sites of chronic inflammation caused by infections with microbes like *Helicobacter pylori* and hepatitis viruses. Noninfectious chronic inflammation such as that caused by asbestos is also associated with tumor development (1–3).

Infectious inflammation is associated with the secretion of several cytokines by innate immune cells in response to pathogen-associated molecular pattern stimuli (4). One of these cytokines is IL-23. IL-23 is a member of the proinflammatory heterodimeric cytokine family and consists of a p19 subunit and a p40 subunit that is shared with IL-12 (5, 6). Whereas IL-12 mainly induces the development of IFN-γ-producing Th1 cells, IL-23 is involved in maintaining the Th17 cells that are generated in response to IL-6 and TGF-β (7–10) and activates memory T cells ($CD44^{high}$ and $CD62L^{low}$) (11). IL-23 also induces the production of the proinflammatory cytokines IL-17 and IL-22 (11, 12). IL-23 is mainly produced by APCs, such as monocytes/macrophages and dendritic cells (DCs)[3] in response to stimulation with TLR2 and 4 ligands, such as peptidoglycan (PGN), LPS, and bacillus Calmette-Guérin cell wall skeleton (BCG-CWS) (13–15).

Recently, the Oft group (16) showed that IL-23 but not IL-12 is overexpressed by macrophages and DCs in human and mouse tumor tissues. They also showed that IL-23 is an important molecule that leads to the up-regulation of IL-17 and the matrix metalloprotease 9, to an increase in angiogenesis, and to a reduction in $CD8^+$ T cell infiltration in the tumor microenvironment (16). Significantly, IL-23p19-deficient mice but not IL-12p35-deficient mice developed chemically induced tumors less frequently than wild-type mice, and tumors transplanted into IL-23 receptor-deficient mice showed reduced growth (16). Furthermore, it was shown that Th17 cells are gradually increased in the tumor microenvironment during tumor development (17) and that IL-17 upregulates the production of a variety of proinflammatory cytokines (18) and proangiogenic factors (19) to promote tumor development (20). Therefore, the activation of the IL-23/IL-17 pathway promotes the incidence and growth of tumors by inducing local inflammatory responses. However, it remains unclear what induces inflammation and IL-23 overproduction in the tumor microenvironment. Notably, peripheral blood cells from patients with lung cancer that had been cultured with TLR stimuli overproduced IL-12/23p40; this response was eliminated in most patients after tumor resection (21). On the basis of these studies, we speculated that the tumor itself produces a factor(s) that promotes IL-23 overproduction. To test our hypothesis, we searched for tumor-secreted

*Department of Molecular Genetics and †Department of Surgery, Osaka Medical Center for Cancer and Cardiovascular Diseases, Osaka, Japan; and ‡Department of Microbiology and Immunology, Hokkaido University Graduate School of Medicine, Sapporo, Japan

Received for publication May 23, 2007. Accepted for publication March 23, 2008.

The costs of publication of this article were defrayed in part by the payment of page charges. This article must therefore be hereby marked *advertisement* in accordance with 18 U.S.C. Section 1734 solely to indicate this fact.

[1] This work was supported by a grant from the Cooperative Link of Unique Science and Technology for Economy Revitalization promoted by the Ministry of Education, Culture, Sports, Science and Technology of Japan and a Grant-in-Aid for Young Scientists from the Ministry of Education, Culture, Sports, Science, and Technology.

[2] Address correspondence and reprint requests to Dr. Norimitsu Inoue, Department of Molecular Genetics, Osaka Medical Center for Cancer and Cardiovascular Diseases, 1-3-3 Nakamichi, Higashinari-ku, Osaka 537-8511, Japan. E-mail address: inoue-no@mc.pref.osaka.jp

[3] Abbreviations used in this paper: DC, dendritic cell; PGN, peptidoglycan; BCG, bacillus Calmette-Guérin; CWS, cell wall skeleton; LDH, lactate dehydrogenase; MCT, monocarboxylate transporter; siRNA, small interfering RNA; Pam_3CSK_4, *N*-palmitoyl-*S*-[2,3-bis(palmitoyloxy)-(2*R*,*S*)propyl]-[*R*]-cysteinyl-[*S*]-seryl-[*S*]-lysl-[*S*]-lysl-[*S*]-lysl-[*S*]-lysine/^{3}HCl; BCECF, 2′,7′-bis-(2-carboxyethyl)-5-(and-6)-carboxyfluorescein/acetoxymethyl ester.

factors that might modulate the production of IL-23 by monocytes/macrophages stimulated with TLR ligands. In this study, we show that lactic acid secreted from tumor cells up-regulates TLR signal-dependent transcription of the IL-23p19 subunit in human and mouse monocytes/macrophages to enhance IL-23 secretion. Therefore, we predict that the lactic acid that is secreted by many tumor cells is a proinflammatory mediator that promotes tumor development.

Materials and Methods

Cell culture

The CADO-LC10 cell line, which was established from a human lung adenocarcinoma (22), was cultured in high glucose DMEM (4.5 mg/ml glucose; Sigma-Aldrich). Human PBMC, human monocytes, mouse splenocytes, the mouse macrophage-like cell line J774.1 (RIKEN cell bank), and the mouse melanoma cell line B16 were cultured in RPMI 1640 (Sigma-Aldrich). All media were supplemented with 10% heat-inactivated FCS, 100 U/ml penicillin, and 100 μg/ml streptomycin. Cells were cultured at 37°C under a 5% CO_2 atmosphere.

Reagents and Abs

We purchased the TLR ligands: PGN of *Staphylococcus aureus* and LPS from Sigma-Aldrich and a synthetic tripalmitoylated lipopeptide, Pam_3CSK_4, from InvivoGen. BCG-CWS was prepared as described previously (23, 24). L-Lactic acid was purchased from Sigma-Aldrich and Wako Pure Chemical and sodium lactate was purchased from WAKO. We used anti-mouse IL-23p19 Ab (G23-8; eBioscience) to neutralize IL-23 activity and rat IgG1 Ab (eBRG1; eBioscience) as an isotype control; both Abs were used at a concentration of 10 μg/ml. We purchased recombinant GM-CSF from PeproTech and anti-GM-CSF receptor α-chain Ab (S-20) from Santa Cruz Biotechnology.

Conditioned medium analysis

Conditioned medium was prepared from CADO-LC10 cells that had been cultured for 3 days. The medium was passed through a 0.22-μm pore size filter (Millipore) and stored at −80°C. For some experiments, the conditioned medium was subjected to molecular size fractionation by using Microcon YM-10 centrifugal filter devices, which separates molecules at the nominal 10-kDa molecular mass cutoff (Millipore). The flow-through fraction (<10 kDa) was supplemented with 10% FCS and the retentate (>10 kDa) was diluted with serum-free culture medium to obtain the original volume. In other experiments, the conditioned medium was treated with 50 μg/ml proteinase K at 37°C for 1 h. To remove proteinase K, the medium was passed through a Microcon YM-10 and the flow-through fraction was used for further experimentation. The control media were subjected to the same treatments as the conditioned media.

To examine how glucose concentrations in the culture medium of CADO-LC10 affects the subsequent enhancing activity of the conditioned medium, we cultured confluent CADO-LC10 cells for 3 days in fresh glucose-free DMEM (Invitrogen) supplemented with 1 or 4.5 mg/ml glucose and 10% FCS. In separate experiments, we inhibited lactic acid production by culturing the CADO-LC10 cells in the presence or absence of 20 mM oxamic acid (Sigma-Aldrich) for 2 days. The pH of the conditioned media and the lactic acid-containing media neutralized with NaOH was measured with a pH meter (Beckman Coulter) at 37°C under a 5% CO_2 atmosphere. L-Lactic acid concentrations in the conditioned media were measured by using a Determiner LA Kit (Kyowamedics). In the enhancing activity analysis, the conditioned media of CADO-LC10 cells described above were added to cells with an equal volume of cell culture media (i.e., 50% of the medium consisted of conditioned medium).

Measurement of cytokines

Human PBMC were isolated from healthy volunteers by using Ficoll-Paque Plus (GE Healthcare Bio-Sciences). Human monocytes were purified from the PBMC by using the MACS system (Miltenyi Biotec) and monocyte isolation kit II (Miltenyi Biotec). To measure human IL-23 production, 1.5×10^5 monocytes were cultured in 96-well tissue culture plates in the presence or absence of lactic acid for 24 h and then treated with 10 μg/ml PGN for 24 h. The IL-23, IL-12/23p40, and IL-6 levels in the culture supernatants were measured by using human IL-23 (Bender MedSystems), human IL-12p40, and human IL-6 (BioSource International) ELISA kits, respectively. To measure mouse IL-23 production, 1.0×10^5 J744.1 cells were stimulated with lactic acid and 10 μg/ml PGN. The measurements of mouse IL-23 production were performed by using a mouse IL-23 ELISA kit (eBioscience).

Mouse splenocytes isolated from an OVA-specific, MHC class II-restricted αβ TCR-transgenic mouse, OT-II (25), were cultured at 5×10^5 cells/well in 96-well tissue culture plates with 0.2 μg/ml $OVA_{323-339}$ peptides (Biosynth International) in the presence or absence of TLR ligands and lactic acid. After 4 days of incubation, the cytokines in the culture supernatants were measured by using IL-17A (R&D Systems) and IFN-γ (BioSource International) ELISA kits. These experiments using animals were conducted according to our institutional guidelines.

Real-time RT-PCR

Total RNA was isolated from cells by using the SV96 Total RNA Isolation System (Promega) according to the manufacturer's instructions, after which it was treated with RNase-free DNase I. cDNA was synthesized at 42°C for 50 min by using oligo$(dT)_{12-18}$ primers and SuperScript III reverse transcriptase in the presence of RNase inhibitor (Invitrogen). Diluted cDNA samples were mixed with a pair of primers derived from human *IL-23p19* or *β-actin* cDNA sequences and PCR was performed by using SYBR Green PCR master mix (Applied Biosystems) and an Applied Biosystems 7500HT sequence detection system. The following PCR primers were designed: for human *IL-23p19*, forward primer, 5′-AGTGTGGAG ATGGCTGTGACC-3′ and reverse primer, 5′-GCTGGGACTGAGGCT TGGAATCTG-3′; for human *IL-12/23p40*, forward primer, 5′-ATGCCGT TCACAAGCTCAAGTATG-3′ and reverse primer, 5′-GAACGCAGAAT GTCAGGGAGAAGT-3′; and for human *β-actin*, forward primer, 5′-TCA CCCACACTGTGCCCATCTACGA-3′ and reverse primer, 5′-CAGCGG AACCGCTCATTGCCAATGG-3′. Copy numbers were calculated from the amount of cDNA cloned into the pGEM-T easy vector (Promega) and normalized to *β-actin*. PCR for mouse *IL-23p19* and *β-actin* was performed by using the TaqMan PCR Core reagent kit, TaqMan probes, and primer sets of the TaqMan Gene Expression assay system (for *IL-23p19*, Mm00518984_m1 and for *β-actin*, Mm00607939_s1; Applied Biosystems). The relative expression of *IL-23p19* was normalized to that of *β-actin* and calculated by using the ΔΔCt method (16, 26).

Luciferase assay

A luciferase reporter plasmid for monitoring *IL-23p19* transcription was constructed as follows. A 6.7-kb fragment of the human *IL-23p19* gene from the *Sac*I site (−6654 bp) to the ATG initiation site that contained the 5′-flanking region and 5′-untranslated region of the gene was amplified by PCR using the RP11-348M3 clone (Research Genetics) as the template. The fragment was then subcloned between the *Sac*I and *Nco*I sites of the pGL3 promoter vector (Promega) to generate the p19–5′ luc vector. We also constructed a reporter gene plasmid containing the 2.7-kb 5′-flanking region of the human *IL-23p19* gene as follows. The p19–5′ luc plasmid was digested with *Sac*I and *Xma*I, treated with T4 DNA polymerase (Takara Bio), and self-ligated. We then inserted the *Xho*I and *Bam*H I fragments of the PGK promoter-driven neomycin resistance gene from pGKEM7-neoW into the *Sal*I and *Bam*H I sites of the plasmid to generate the p19–5′ 2.7k luc neo vector. The luciferase reporter plasmid for monitoring NF-κB activity was constructed as follows. The following synthetic oligonucleotides were annealed: 5′-TCGAGAAATGGGGACTTTCCGC TGGGGACTTTCCGCAAACCGC-3′ and 5′-GGTTTGCGGAAAGTCC CCAGCGGAAAGTCCCCATTTC-3′ (the underlined sequences indicate canonical NF-κB binding sites). The annealed oligonucleotides were then subcloned together with a *Sac*II/*Nco*I fragment of the minimal promoter sequence of the pNF-κB-Luc vector (Stratagene) between *Xho*I and *Nco*I sites of the pGL3 promoter vector containing the PGK promoter-driven neomycin resistance gene to generate the pGL3–2κB luc neo vector. J774.1 cells were then transfected with the p19-5′ luc vector and pGKEM7-neoW, the p19-5′ 2.7k luc neo vector, or pGL3–2κB luc neo vector by using FuGENE 6 (Roche) according to the manufacturer's instructions. The transfected cells were selected with 200 μg/ml G418. The cells were seeded in 96-well tissue culture plates at 1×10^5 cells/well and incubated with stimulants for 24 h as described above. After incubation, the cells were lysed with GloLysis buffer (Promega) and the luciferase activity was measured by using the Bright-Glo luciferase assay system (Promega) and a Mithras LB940 multimode reader (Berthold Technologies).

Small interfering RNA (siRNA)

We purchased *SMART*pool siRNA reagents for the human *LDHA* gene from Dharmacon and the Allstars negative control siRNA rhodamine from Qiagen. CADO-LC10 cells were transfected with siRNA (73 nM) by using XtremeGENE siRNA Transfection Reagent (Roche) according to the manufacturer's instructions. This transfection procedure was repeated on the second day to increase the RNA interference efficiency. On the fourth day,

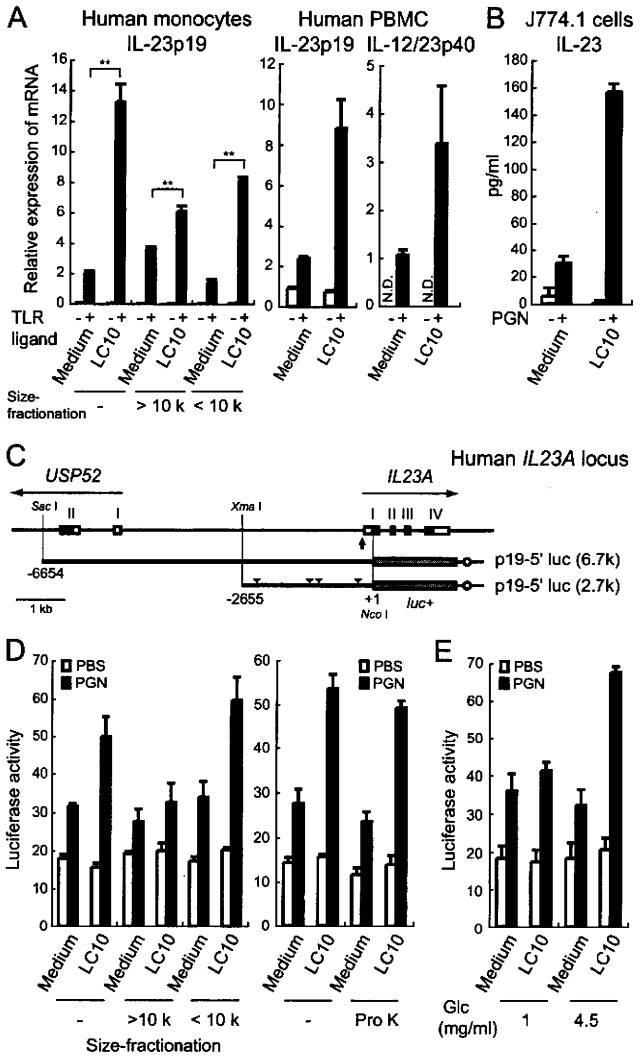

FIGURE 1. Tumor cell-conditioned medium enhances IL-23 expression in TLR ligand-stimulated monocytes/macrophages. *A*, Conditioned medium of the lung adenocarcinoma cell line CADO-LC10 enhances the TLR ligand-induced *IL-23p19* mRNA expression in human monocytes/macrophages (*left*). Human monocytes were stimulated with 10 μg/ml PGN (■) or PBS (□) in the presence (LC10) or absence (Medium) of 50% of the conditioned medium for 4 h. The conditioned medium was also fractionated according to molecular size, with the cutoff being at the nominal 10-kDa molecular mass (*left*). Human PBMC were stimulated with 5 μg/ml BCG-CWS in the presence or absence of the conditioned medium (*middle* and *right*). The relative expression of *IL-23p19* (*left* and *middle*) and *IL-12/23p40* (*right*) mRNA was measured by real-time RT-PCR and normalized to *β-actin* expression. N.D., Not detected. *B*, J774.1 cells were stimulated with 10 μg/ml PGN for 24 h in the presence or absence of the conditioned medium and the IL-23 that was secreted was measured by ELISA. *C*, Schematic representation of the human *IL23A* gene locus and two luciferase reporter genes carrying the 5′-flanking regions of the *IL-23p19* gene. The position from the translation start site (+1) is indicated in each construct. Shown are the untranslated regions (□), the coding region of *IL-23p19* and the *USP52* exon (■), the *luciferase* gene (▨), the SV40 late poly(A) signal (○), and the TATA box sequence (arrow). The arrowheads indicate putative NF-κB binding sites (−2311 to −2302, −1261 to −1252, −1049 to −1040, and −256 to −245) in the 2.7-kb 5′-flanking region. *D*, J774-p19-5′ luc cells were stimulated with 10 μg/ml PGN in the presence of the whole conditioned medium or the size-fractionated conditioned medium (*left*) or conditioned medium that had been treated with 50 μg/ml proteinase K (Pro K) for 1 h (*right*). Luciferase activity was then measured. *E*, Conditioned media were prepared from CADO-LC10 cells cultured in medium containing 1 or 4.5 mg/ml glucose (Glc). The control media (Medium) were subjected to the same treatments as the conditioned media (LC10). These media were added at 50% to determine the enhancing activity. The data represent mean values ± SD ($n = 3$). **, $p < 0.01$.

the cells were collected and plated at 1.4×10^6 cells/well in 12-well plates. After incubation for 24 h, we collected the conditioned medium and incubated the cells further for 24 h. The collected media were combined and used for further analysis. The expression of LDHA in siRNA-transfected CADO-LC10 cells was evaluated by performing semiquantitative RT-PCR and Western blotting. The following PCR primers were used: for human *LDHA*, forward primer, 5′-GCACGTCAGCAAGAGGGAGAAAG-3′ and reverse primer, 5′-AGGTAACGGAATCGGGCTGAATC-3′ and for human *β-actin*, forward primer, 5′-GCGGGAAATCGTGCGTGACATT-3′ and reverse primer, 5′-GATGGAGTTGAAGGTAGTTTCGTG-3′. Anti-LDHA (N-14; Santa Cruz Biotechnology) and anti-β-tubulin (TUB 2.1; Sigma-Aldrich) Abs were used for Western blotting. The expression levels of proteins were calculated by using Image J software (http://rsb.info.nih.gov/ij/) and were normalized to those of β-tubulin expression.

Measurement of intracellular pH

Intracellular pH was measured by using BCECF/AM (Invitrogen) (27). Fluorescence at 535 nm with excitation at 485 and 388 nm was measured for 0.1 s every 30 s after adding lactic acid or hydrochloric acid (WAKO) by using an ARVO MX 1420 multilabel counter (PerkinElmer).

Purification of tumor-infiltrating immune cells

Tumor-infiltrating immune cells were purified from tumors formed by B16 melanoma cells in C57BL/6 mice by using CD45 MACS MicroBeads (Miltenyi Biotec) as described previously (28). The purified cells were stained with FITC-conjugated anti-CD45.2 (104; eBioscience), FITC-conjugated anti-CD11b (M1/70; eBioscience), and PE-conjugated anti-CD11c (HL3; BD Biosciences) and examined by using the FACSCalibur system (BD Biosciences).

Statistical analyses

In measurement of cytokines, real-time PCR, and luciferase assay, data represent mean values ± SD of triplicate stimulations. Differences between groups were analyzed for statistical significance by the Student *t* test. Representative data from at least two independent experiments are shown in the figures.

Results

Tumor cell-conditioned medium enhances TLR ligand-induced IL-23p19 *expression in monocytes/macrophages*

To determine whether tumor-secreted factors might modulate the TLR ligand-stimulated production of IL-23 by monocytes/macrophages, we first generated medium conditioned by the lung adenocarcinoma cell line CADO-LC10. Monocytes isolated from normal human PBMC were then stimulated with PGN in the presence (LC10) or absence (medium) of the conditioned medium. PGN induced *IL-23p19* transcription in human monocytes/macrophages and the transcription was significantly increased by the presence of the conditioned medium (Fig. 1*A*, *left*). The conditioned medium alone did not induce *IL-23p19* transcription in unstimulated monocytes/macrophages (Fig. *1A*, *left*). Similar results were obtained for PBMC stimulated with BCG-CWS (Fig. 1*A*, *middle*).

We then size-fractionated the conditioned medium and the control medium into two fractions bearing the >10-kDa or <10-kDa molecules and performed the same experiment described above. The PGN-stimulated expression of *IL-23p19* in the monocytes/macrophages was more strongly enhanced by the lower molecular mass fraction (5.9-fold) than by the higher molecular mass fraction (1.7-fold) (Fig. 1*A*, *left*). Thus, it appears that the tumor cells secrete a small molecule that augments TLR ligand-induced IL-23p19 expression in monocytes/macrophages.

We also examined the effect of the conditioned medium on the transcriptional expression of *IL-12/23p40* in human PBMC. Although the unfractionated medium and the higher molecular mass

fraction clearly enhanced the transcription of *IL-12/23p40*, the lower molecular mass fraction did not (Fig. 1*A*, *right*, and data not shown). The enhancement of IL-12/23p40 expression was significantly inhibited by the anti-GM-CSF receptor α-chain Ab, suggesting that GM-CSF in the conditioned medium mainly enhanced IL-12/23p40 expression (data not shown).

The conditioned medium also enhanced the PGN-induced secretion of IL-23 by the mouse macrophage-like cell line J774.1 (Fig. 1*B*).

The conditioned medium enhances IL-23p19 *promoter activity*

To examine the effect of the conditioned medium on *IL-23p19* gene promoter activity, we performed a luciferase reporter assay using p19-5′ luc, which is a luciferase reporter plasmid containing the 6.7-kb 5′-flanking DNA region of the human *IL-23p19* gene (Fig. 1*C*). We first established several stable J774.1 cell lines that contained the reporter plasmid p19-5′ luc (J774-p19–5′ luc cells). When these cell lines were stimulated with PGN, *IL-23p19* promoter activity was increased (Fig. 1*D*, *left*). A further increase was observed when the cells were treated with PGN in the presence of the conditioned medium (Fig. 1*D*, *left*). Here again, the lower molecular mass fraction of the conditioned medium was proficient in stimulating *IL-23p19* promoter activity (Fig. 1*D*, *left*). We also generated additional luciferase reporter cells (J774-p19-5′ 2.7k luc) from p19-5′ 2.7k luc that contained only the 2.7-kb 5′-flanking region of the human *IL-23p19* gene (Fig. 1*C*). The reporter activity of this plasmid in J774.1 cells was increased by TLR stimuli (BCG-CWS and PGN) and this effect was further increased by the conditioned medium (data not shown).

Thus, the conditioned medium augments the stimulatory effect of TLR ligands on *IL-23p19* promoter activity.

Characterization of the small molecule in the conditioned medium responsible for the increase in TLR-stimulated IL-23p19 *promoter activity*

To identify the small molecule in the conditioned medium, we subjected the conditioned medium to further molecular size fractionation that separated the molecules at the nominal molecular mass of 500 Da. The <500-Da fraction, but not the >500-Da fraction, increased the *IL-23p19* promoter activity in TLR ligand-stimulated J774-p19-5′ luc (data not shown). The enhancing activity of the entire conditioned medium was not diminished by treatment with proteinase K (Fig. 1*D*, *right*) or heat treatment at 90°C for 10 min (data not shown). Thus, it appeared that the tumor-secreted small molecule we were interested in would not be a protein or peptide.

Interestingly, we found that the enhancing activity of the conditioned medium varied depending on whether the medium was obtained from tumor cell cultures in DMEM (2.4 ± 0.21), RPMI 1640 (1.6 ± 0.06), or MEM (1.0 ± 0.07). DMEM was better than RPMI 1640 and MEM had no enhancing effect at all. DMEM, RPMI 1640, and MEM contain different concentrations of glucose, namely, 4.5, 2, and 1 mg/ml, respectively. To investigate whether the glucose concentration does indeed affect the subsequent enhancing activity of the conditioned medium, we generated conditioned media from CADO-LC10 cells cultured for 3 days in DMEM supplemented with low (1 mg/ml) or high (4.5 mg/ml) concentrations of glucose. The conditioned medium prepared in high glucose DMEM enhanced the TLR ligand-stimulated *IL-23p19* promoter activity in J774-p19-5′ luc cells, unlike the conditioned medium prepared in low glucose DMEM (Fig. 1*E*). A high concentration of glucose alone had no effect (Fig. 1*E*). Glucose was metabolized to pyruvic acid, which is catalyzed by lactate dehydrogenase (LDH) to generate lactic acid. Because tumor cells show up-regulated glycolysis, even under aerobic conditions, they generally secrete large amounts of lactic acid into the culture medium (29–31). Indeed, the conditioned media of CADO-LC10 cells cultured in 4.5 or 1 mg/ml glucose were found to contain 26.4 and 7.8 mM lactic acid, respectively (final concentrations of 13.2 and 3.9 mM in our assay). Therefore, we hypothesized that lactic acid may be the most likely candidate tumor cell-secreted factor that enhances TLR ligand-stimulated *IL-23p19* transcription.

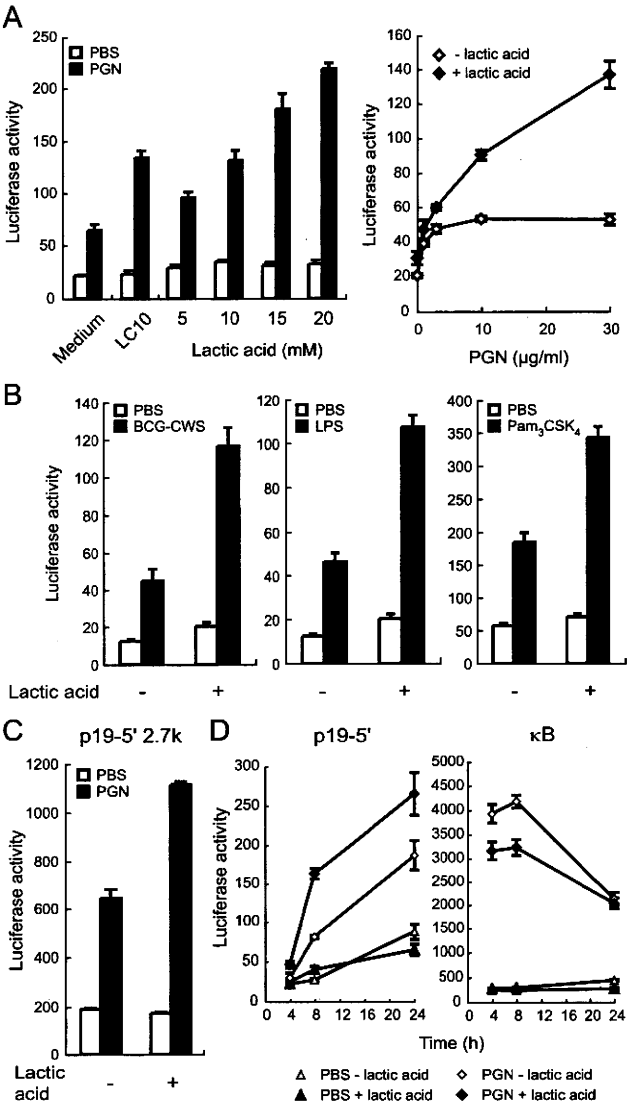

FIGURE 2. Lactic acid enhances TLR ligand-induced human *IL-23p19* promoter activity. *A*, J774-p19-5′ luc cells were stimulated with 10 μg/ml PGN in the presence of 0 (Medium), 5, 10, 15, or 20 mM lactic acid (*left*) or with 0, 2.5, 5, 10, or 30 μg/ml PGN in the presence of 15 mM lactic acid (*right*). *B*, J774-p19-5′ luc cells were stimulated with 10 μg/ml BCG-CWS (*left*), 100 ng/ml LPS (*middle*), or 100 ng/ml Pam_3CSK_4 (*right*) in the presence or absence of 15 mM lactic acid. *C*, J774-p19-5′ 2.7k luc cells were stimulated with 10 μg/ml PGN in the presence or absence of 15 mM lactic acid. *D*, J774-p19-5′ luc cells (*left*) and J774-2κB luc cells (*right*) were stimulated with 10 μg/ml PGN in the presence or absence of 15 mM lactic acid. After incubation for 4, 8, and 24 h, the cells were lysed and their luciferase activities were measured. The data represent mean values ± SD ($n = 3$).

Lactic acid in the conditioned medium enhances the IL-23p19 *gene expression induced by TLR ligands*

To examine whether lactic acid indeed enhances the *IL-23p19* gene expression induced by TLR ligands, J774-p19-5′ luc cells were stimulated with PGN in the presence of lactic acid. The luciferase activity in J774-p19-5′ luc cells was increased by lactic acid in a dose-dependent manner (Fig. 2*A*, *left*) and this enhancing

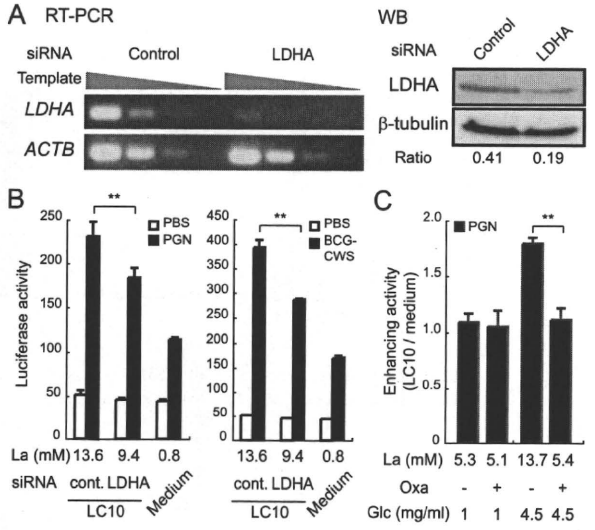

FIGURE 3. Inhibiting the production of lactic acid blocks the enhancing activity of the conditioned medium. *A*, CADO-LC10 cells were transfected with siRNA for the human *LDHA* gene (LDHA) or negative control siRNA (Control). The inhibitory effect of *LDHA* siRNA was assessed by semi-quantitative RT-PCR (*left*) and Western blotting (WB; *right*). cDNA templates prepared from siRNA-transfected CADO-LC10 cells were serially diluted (1, 0.1, 0.01, and 0.001) and amplified with *LDHA* and *β-actin* (*ACTB*) primers. Cell lysates of siRNA-transfected CADO-LC10 cells were immunoblotted with anti-LDHA or anti-β-tubulin Abs. The normalized protein expression levels of LDHA are shown below the picture. *B*, J774-p19-5′ luc cells were cultured with the conditioned media prepared from siRNA-transfected CADO-LC10 cells in the presence of 10 μg/ml PGN (*left*) or 10 μg/ml BCG-CWS (*right*) for 24 h. *C*, Alternatively, CADO-LC10 cells were incubated in low or high glucose DMEM with 20 mM oxamic acid (Oxa), an inhibitor of LDH. J774-p19-5′ luc cells were cultured with these conditioned media in the presence of 10 μg/ml PGN for 24 h. The data indicate the relative enhancing activity of CADO-LC10 conditioned medium over that of the average of control medium. The concentration of lactic acid (La) in each conditioned medium was measured in *B* and *C*. The data represent mean values ± SD ($n = 3$). **, $p < 0.01$.

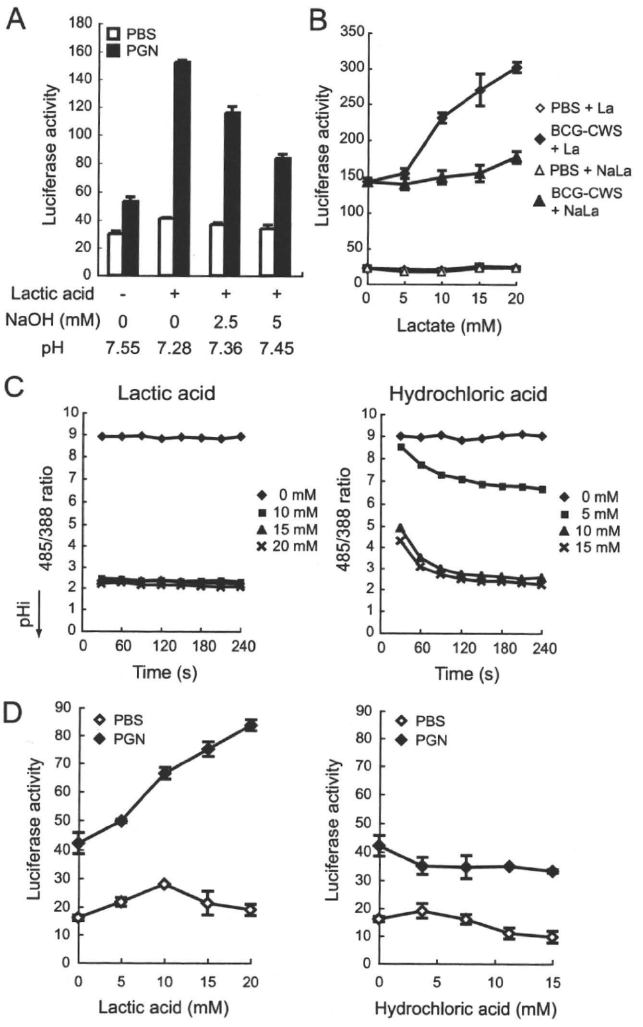

FIGURE 4. The enhancing activity of lactic acid is dependent on the pH of the medium. *A*, pH of the medium containing 15 mM lactic acid (pH 7.28) was adjusted to 7.36 and 7.45 with 2.5 and 5 mM NaOH, respectively. J774-p19-5′ luc cells were stimulated with 10 μg/ml PGN in the presence of these media. *B*, J774-p19-5′ luc cells were stimulated with 10 μg/ml BCG-CWS in the presence of 0, 5, 10, 15, or 20 mM lactic acid (La) or sodium lactate (NaLa). *C*, BCECF-loaded J774-p19-5′ luc cells were incubated with 0, 10, 15, or 20 mM lactic acid (*left*) or 0, 5, 10, or 15 mM hydrochloric acid (*right*). Intracellular pH (pHi) was detected by examining the fluorescent pH dye BCECF every 30 s as described in *Materials and Methods*. The ratio of fluorescence at 535 nm after excitation at 485 nm/388 nm was calculated. *D*, J774-p19-5′ luc cells were stimulated with 10 μg/ml PGN in the presence of various concentrations of lactic acid (*left*) or hydrochloric acid (*right*). After a 24-h incubation, the cells were lysed and the luciferase activity was measured. The data represent mean values ± SD ($n = 3$).

effect was observed at all concentrations of PGN (Fig. 2*A*, *right*). However, lactic acid alone had no detectable effect in this assay (Fig. 2*A*, *left*, □). Lactic acid at 10 mM was as effective as the conditioned medium, which contained 27.3 ± 1.09 mM lactic acid (final concentration of 13.7 ± 0.55 mM in our assay; Fig. 2*A*, *left*). The enhancing activity of lactic acid was also observed with cells stimulated with not only PGN but also other TLR ligands, namely, BCG-CWS, LPS, and Pam_3CSK_4 (Fig. 2*B*).

We next examined the region in the *IL-23p19* promoter that was responsive to lactic acid by using J774-p19-5′ 2.7k luc cells. DNA elements responsible for this enhancing activity of lactic acid like the conditioned medium were detected in a 2.7-kb 5′-flanking region of the human *IL-23p19* gene (Fig. 2*C*). Searching of a TRANSFAC database (32) with the TFSEARCH program version 1.3 (http://www.rwcp.or.jp/papia/) revealed four predicted NF-κB binding sites in a 2.7-kb 5′-flanking region (Fig. 1*B*, arrowheads). However, when we constructed J774.1 cells transfected with a luciferase reporter construct carrying canonical NF-κB binding sites and tested their responses to TLR ligands in the presence or absence of lactic acid, we did not observe any enhancing activity (Fig. 2*D*).

To test whether the lactic acid secreted from the tumor cells is indeed responsible for augmenting the TLR ligand-induced *IL-23p19* promoter activity, we inhibited the production of lactic acid from CADO-LC10 cells with *LDHA*-specific siRNA. The expression of *LDHA* mRNA (Fig. 3*A*, *left*) and protein (Fig. 3*A*, *right*) in *LDHA* siRNA-transfected cells was reduced to <10 and 50% of that of control siRNA-transfected cells, respectively. We examined enhancing activity using these conditioned media (Fig. 3*B*). Alternatively, we inhibited the LDH activity by adding oxamic acid, an inhibitor of LDH (Fig. 3*C*). Both treatments significantly reduced the concentration of lactic acid in the conditioned medium and this was matched with a decreased ability of the conditioned medium to enhance TLR ligand-stimulated *IL-23p19* promoter activity (Fig. 3, *B* and *C*). Thus, the lactic acid secreted by the tumor cells was largely responsible for the enhancing effect of the conditioned medium.

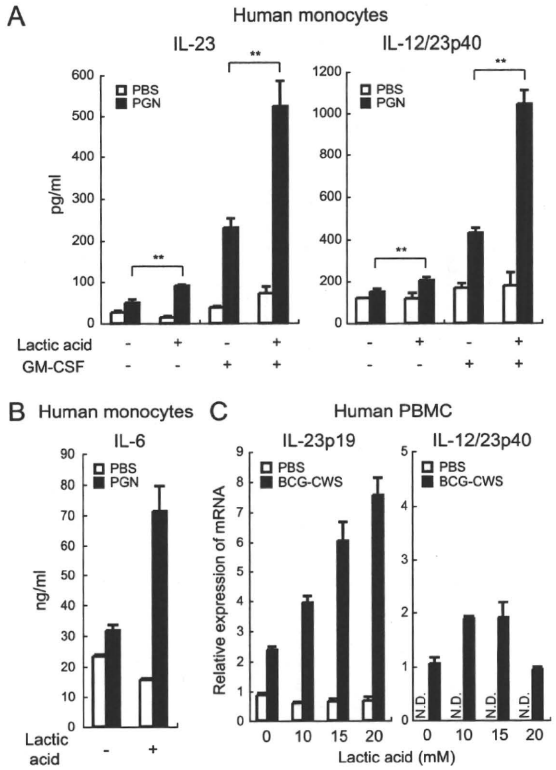

FIGURE 5. Lactic acid enhances proinflammatory cytokine production by TLR ligand-stimulated human primary monocytes/macrophages. *A*, Human monocytes were cultured for 24 h in the presence or absence of 15 mM lactic acid with or without 5 unit/ml GM-CSF. The cells were then stimulated with 10 μg/ml PGN for 24 h and the supernatants were collected. The IL-23 heterodimer and IL-12/23p40 concentrations were measured by ELISA. *B*, Human monocytes were cultured for 24 h in the presence or absence of 15 mM lactic acid. The cells were then stimulated with 10 μg/ml PGN for 24 h and the IL-6 concentrations of the supernatants were measured by ELISA. *C*, Human PBMC were stimulated with 5 μg/ml BCG-CWS in the presence of 0, 10, 15, or 20 mM lactic acid. After 4 h, *IL-23p19* (*left*) and *IL-12/23p40* (*right*) transcripts were measured by real-time RT-PCR. Relative expression of these transcripts was normalized to *β-actin* expression. N.D., Not detected. The data represent mean values ± SD ($n = 3$). **, $p < 0.01$.

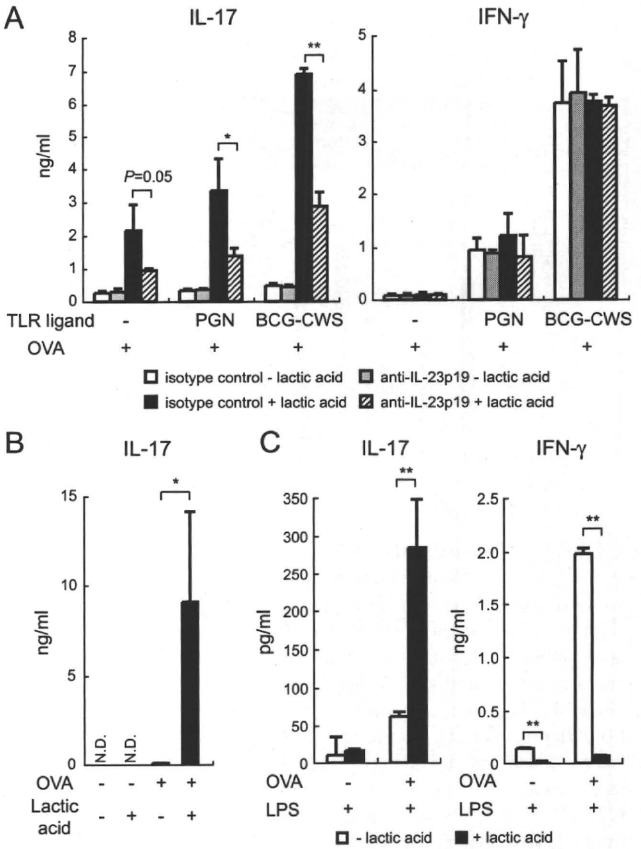

FIGURE 6. The IL-17 production by Ag-stimulated mouse splenocytes is augmented by lactic acid. *A*, Splenocytes from OT-II mice were stimulated with (■ and ▨) or without (□ and ▩) 15 mM lactic acid and PBS, 10 μg/ml PGN, or 1 μg/ml BCG-CWS. Anti-IL-23p19 Ab (▩ and ▨) or isotype control rat IgG1 (□ and ■) was also present, along with 0.2 μg/ml $OVA_{323-339}$ peptide. *B*, Splenocytes from OT-II mice were stimulated with or without 0.2 μg/ml OVA peptide and 15 mM lactic acid. *C*, Splenocytes from OT-II mice were stimulated with 100 ng/ml LPS and 0.2 μg/ml OVA peptide in the presence (■) or absence (□) of 15 mM lactic acid. The supernatants were collected after 4 days and the IL-17 and IFN-γ concentrations were measured by ELISA. N.D., Not detected. The data represent mean values ± SD ($n = 3$). *, $p < 0.05$ and **, $p < 0.01$.

Pathway involved in the enhancing activity of lactic acid

Lactate anions are transported together with protons into cells by monocarboxylate transporters (MCTs) in a pH-dependent manner (33). Therefore, to examine whether the enhancing activity of lactic acid depends on the pH of the medium, we incubated J774-p19-5′ luc cells with 15 mM lactic acid in the presence of NaOH, which altered the pH of the medium (Fig. 4*A*). The enhancing activity of lactic acid was decreased in a NaOH dose-dependent manner. Furthermore, sodium lactate did not show any enhancing activity (Fig. 4*B*). The intracellular pH of the cells decreased rapidly upon incubation with lactic acid (Fig. 4*C*, *left*), suggesting that protons were transported into the cells along with lactic acid. However, in contrast to lactic acid, hydrochloric acid, which also decreased the intracellular pH, had no enhancing effect (Fig. 4, *C*, *right*, and *D*). These results suggest that only the lactate anion in its transportable state, but not the neutralized lactate anion or proton, was responsible for the enhancing activity.

Lactic acid enhances secretion of proinflammatory cytokines by human monocytes/macrophages

The IL-23p19 subunit is covalently linked to the IL-12/23p40 subunit to form an IL-23 heterodimer. The heterodimer is secreted by monocytes/macrophages/DCs stimulated with TLR ligands (5, 34). To investigate whether lactic acid enhances IL-23 secretion, human monocytes were stimulated with PGN in the presence of lactic acid for 24 h (Fig. 5*A*, *left*). The secretion of IL-23 was enhanced 1.8-fold by lactic acid. When GM-CSF was only present, IL-23 secretion was elevated 4.7-fold. When lactic acid and GM-CSF were both present, IL-23 secretion was enhanced 10.6-fold. Similarly, the PGN-induced secretion of IL-12/23p40 was slightly increased by lactic acid but synergistically enhanced by the further addition of GM-CSF (Fig. 5*A*, *right*). These results indicate that lactic acid and GM-CSF cooperate to stimulate TLR ligand-induced IL-23 and IL-12/23p40 production by human monocytes/macrophages. Furthermore, lactic acid also enhanced the secretion of another proinflammatory cytokine, IL-6, from human monocytes/macrophages stimulated with the TLR ligand (Fig. 5*B*).

We also observed that BCG-CWS increased *IL-23p19* transcription in PBMC, and like the conditioned medium (Fig. 1*A*, *middle*), lactic acid significantly enhanced this response in a dose-dependent manner (Fig. 5*C*, *left*). Conversely, lactic acid did not increase *IL-12/23p40* transcription (Fig. 5*C*, *right*), suggesting that lactic acid specifically acts on *IL-23p19* transcription.

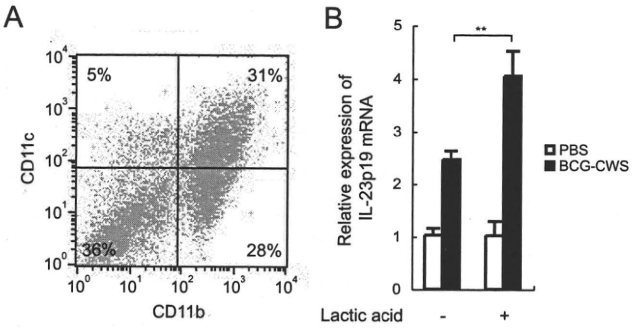

FIGURE 7. Lactic acid enhances the expression of *IL-23p19* mRNA in tumor-infiltrating immune cells. *A*, Tumor-infiltrating CD45-positive cells were purified from tumors formed by B16 mouse melanoma cells and stained for CD11b and CD11c. The stained cells were analyzed by FACS. *B*, One hundred thousand tumor-infiltrating immune cells (CD45-positive cells, 86%) were stimulated with 10 μg/ml BCG-CWS in the presence or absence of 15 mM lactic acid. After 4 h, the expression of *IL-23p19* and *β-actin* transcripts was measured by TaqMan RT-PCR. Relative expression was normalized to that of *β-actin*. The data represent mean values ± SD ($n = 3$). **, $p < 0.01$.

Lactic acid enhances the IL-23/IL-17 pathway

Because lactic acid further enhanced TLR-stimulated IL-23 production, we predicted that lactic acid should enhance IL-23 production from APCs stimulated with TLR ligand, leading to increased IL-17 production by IL-17-producing T cells. We then used OT-II-transgenic mice, which have $OVA_{323-339}$ peptide-specific T cells (25). In the presence of the OVA peptide, we examined the effect of lactic acid on the IL-17 production of OT-II mouse splenocytes that had been stimulated with the TLR ligand (PGN or BCG-CWS) for 4 days. Lactic acid remarkably enhanced the secretion of IL-17 induced by PGN and BCG-CWS (Fig. 6*A*, *left*, □ and ■). Anti-IL-23p19 Ab significantly inhibited the lactic acid-induced enhancement of IL-17 production (Fig. 6*A*, *left*, ■ and ▨). This result indicates that lactic acid indeed stimulates APCs to produce IL-23, which then drives peptide-activated T cells to produce IL-17. Interestingly, in the presence of the peptide, lactic acid induced IL-17 production even without the TLR ligand and this effect was inhibited by the anti-IL-23p19 Ab (Fig. 6, *A*, *left*, and *B*). The peptide or lactic acid alone rarely induced IL-17 production by splenocytes (Fig. 6*B*).

We also examined the effect of lactic acid on the secretion of IFN-γ (Fig. 6*A*, *right*). When the TLR ligand was present along with the peptide, the splenocytes produced IFN-γ. However, lactic acid did not potentiate IFN-γ production under these conditions (Fig. 6*A*, *right*, □ and ■). In contrast to IL-17 production, lactic acid did not induce IFN-γ production when the TLR ligand was absent (Fig. 6*A*, *right*). Notably, the effect of lactic acid on IFN-γ production was different when the TLR ligand was replaced by LPS. Although lactic acid potentiated IL-17 production by splenocytes irrespective of the ligand used for stimulation (Fig. 6*C*, *left*), it severely inhibited IFN-γ production (Fig. 6*C*, *right*).

Lactic acid enhances the expression of IL-23p19 *mRNA in tumor-infiltrating immune cells*

Many immune cells infiltrate the tumor microenvironment and induce local inflammation in and around the tumor. We examined whether tumor-infiltrating immune cells actually have the ability to express a high amount of IL-23 in response to lactic acid. We purified CD45-positive cells (CD11b- and/or CD11c-positive cells, 64%) that had infiltrated the tumors formed by B16 melanoma cells (Fig. 7*A*). These cells were stimulated with BCG-CWS and lactic acid for 4 h. The level of *IL-23p19* transcripts significantly increased in the presence of lactic acid (Fig. 7*B*). This result suggests that lactic acid also enhances the production of IL-23 in tumor-infiltrating immune cells, probably in macrophages and/or DCs.

Discussion

Tumor-secreted lactic acid enhances TLR ligand-dependent IL-23 expression in monocytes/macrophages

In this study, we sought to elucidate the mechanisms that induce immune cells in the tumor microenvironment to produce proinflammatory cytokines such as IL-23. We also asked, how does the tumor induce chronic inflammation without being attacked by the immune cells? We found that many tumor cell lines secrete factors that enhance TLR ligand-stimulated *IL-23p19* transcription and IL-23 secretion by human and mouse monocytes/macrophages (Fig. 1*A* and data not shown). We clarified that the main factor responsible for this effect is a molecule smaller than 500 Da that is protease resistant, heat stable, and only secreted from tumor cell lines when they are cultured in high glucose medium (Fig. 1, *D* and *E*, and data not shown). We then discovered that this molecule is lactic acid (Figs. 2–5). Lactic acid increased the production of proinflammatory cytokines, IL-23, and IL-6 from human monocytes (Fig. 5).

GM-CSF also enhanced TLR ligand-induced IL-23 and IL-12/23p40 production (Fig. 5). GM-CSF is secreted by many tumor cells as well as CADO-LC10 cells (35) and increases the expression of TLR2 (36). We suggest that tumor-secreted GM-CSF and lactic acid cooperate to increase IL-23 production following TLR2 ligand stimulation.

Predicted lactic acid signaling pathway

Although lactic acid is completely ionized, even under neutralized conditions (37), the neutralization of lactic acid suppressed its ability to enhance *IL-23p19* promoter activity in a pH-dependent manner (Fig. 4*A*). Moreover, neither sodium lactate nor acidification with hydrochloric acid enhanced *IL-23p19* transcription (Fig. 4, *B* and *D*). Lactate anions are transported together with protons through MCTs and a pH gradient is necessary for effective transport of lactic acid into cells (33). Therefore, we predict that lactic acid transported into monocytes/macrophages by MCTs may be recognized by an intracellular sensor that, along with the TLR signal, activates the *IL-23p19* promoter.

We found that DNA elements responsible for the enhancing activity of lactic acid are localized in the 2.7-kb 5′-flanking region of the human *IL-23p19* gene (Fig. 2*C*). We found four predicted NF-κB binding sites in this region (Fig. 1*C*). Although NF-κB signaling plays an important role in the TLR signaling pathway (4), lactic acid did not enhance the luciferase activity of a reporter vector carrying canonical NF-κB-binding elements (Fig. 2*D*). Therefore, the lactic acid signal pathway may be independent of the NF-κB pathway.

Lactic acid is not only a terminal metabolite of glycolysis but also a proinflammatory mediator

In most normal mammalian cells, the metabolism from glucose to lactate is inhibited by the presence of oxygen, which leads to the oxidization of pyruvate to CO_2 and H_2O in the mitochondria. However, in cancer cells, glycolysis is up-regulated, even in aerobic conditions, a phenomenon known as the "Warburg effect" or "aerobic glycolysis" (29, 30). This results in the production of large amounts of lactic acid and the accumulation of lactic acid in the microenvironment of many cancer cell types (31). High concentrations of lactate in solid tumors such as cervical carcinoma

(10.0 ± 2.9 μmol/g or >8.3 μmol/g) and head and neck cancer (>7.1 μmol/g) are associated with higher frequencies of distant metastasis (31, 38–40). Moreover, low lactate tumors in primary lesions are associated with longer disease-free survival than high lactate tumors. In addition, when the LDHA activity that induces the metabolism of pyruvate to lactate is suppressed, the tumorigenicity is severely diminished (41).

In this study, we showed that lactic acid enhances the expression of IL-23p19 in tumor-infiltrating immune cells activated by TLR stimuli (Fig. 7) and in splenocytes in the presence of Ag stimulus (data not shown) and induces the Ag- and IL-23-dependent secretion of IL-17 from splenocytes (Fig. 6). Significantly, we detected this IL-23-dependent enhancing activity even when TLR ligands were absent. Since lactic acid alone did not induce IL-23 production in the absence of Ag stimulation, we predicted that an interaction between APCs and T cells mediated by Ag and lactic acid causes IL-23-dependent IL-17 production in the absence of the TLR ligand. We observed that lactic acid severely inhibited IFN-γ production by Ag-stimulated splenocytes treated with LPS (Fig. 6*C*, *right*). The Kreutz group (42) reported that lactic acid represses the secretion of IL-12p70 by LPS-stimulated DCs. Therefore, lactic acid may inhibit IFN-γ production by suppressing the IL-12p70 production of monocytes/macrophages. In contrast, lactic acid did not affect IFN-γ production of Ag-stimulated splenocytes treated with PGN or BCG-CWS (Fig. 6*A*, *right*), because it is assumed that PGN and BCG-CWS do not stimulate IL-12p70 production by monocytes/macrophages (14). These results suggest that upon antigenic stimulation of T cells, lactic acid mediates the activation of the IL-23/IL-17 pathway rather than the induction of IFN-γ-producing Th1 cells. We predict that lactic acid derived from tumor cells may induce inflammation but not the infiltration of CTLs in the tumor microenvironment, even in the absence of TLR ligand stimuli from microbial infections, and that inflammation promotes angiogenesis and tumor development.

The Kreutz group (42, 43) also reported that lactic acid down-regulates the cytokine production and proliferation of CTLs. Furthermore, the Murray group (44) showed that MCT1 inhibitors, which inhibit the transport of lactic acid, suppress T lymphocyte proliferation. These groups suggested that a high concentration of extracellular lactic acid or inhibition of lactic acid excretion might cause intracellular accumulation of lactic acid with consequent disturbance of T cell metabolism and function. In contrast, our results indicate that lactic acid up-regulates *IL-23p19* transcription in monocytes/macrophages.

In conclusion, our results show that lactic acid acts as a novel tumor-derived factor that strongly induces the IL-23/IL-17 proinflammatory pathway without inducing Th1 responses. Thus, the production and excretion of lactic acid appears to be not only essential for the proliferation of tumor cells with up-regulated glycolysis, but also for the induction of inflammation in the tumor microenvironment, which promotes tumor progression. Therefore, lactic acid and the lactic acid/IL-23 signal pathway may be an attractive target for treating tumors.

Acknowledgments

We thank K. Kawata, T. Yasuda, and C. Kozai in our laboratory for technical assistance and Dr. M. Saio (Gifu University, Gifu, Japan) for technical support. We also thank Drs. K. Toyoshima (RIKEN, Yokohama, Japan) and I. Azuma (Muroran Institute of Technology, Muroran, Japan) for providing BCG-CWS, Dr. W. R. Heath (The Walter and Eliza Hall Institute of Medical Research, Parkville, Australia) for providing OT-II mice, and Drs. J. Takeda and K. Yusa (Osaka University, Suita, Japan) for providing pGKEM7-neoW.

Disclosures

The authors have no financial conflict of interest.

References

1. de Visser, K. E., A. Eichten, and L. M. Coussens. 2006. Paradoxical roles of the immune system during cancer development. *Nat. Rev. Cancer* 6: 24–37.
2. Karin, M., T. Lawrence, and V. Nizet. 2006. Innate immunity gone awry: linking microbial infections to chronic inflammation and cancer. *Cell* 124: 823–835.
3. Balkwill, F., K. A. Charles, and A. Mantovani. 2005. Smoldering and polarized inflammation in the initiation and promotion of malignant disease. *Cancer Cell* 7: 211–217.
4. Akira, S., S. Uematsu, and O. Takeuchi. 2006. Pathogen recognition and innate immunity. *Cell* 124: 783–801.
5. Oppmann, B., R. Lesley, B. Blom, J. C. Timans, Y. Xu, B. Hunte, F. Vega, N. Yu, J. Wang, K. Singh, et al. 2000. Novel p19 protein engages IL-12p40 to form a cytokine, IL-23, with biological activities similar as well as distinct from IL-12. *Immunity* 13: 715–725.
6. Hunter, C. A. 2005. New IL-12-family members: IL-23 and IL-27, cytokines with divergent functions. *Nat. Rev. Immunol.* 5: 521–531.
7. Veldhoen, M., R. J. Hocking, C. J. Atkins, R. M. Locksley, and B. Stockinger. 2006. TGF-β in the context of an inflammatory cytokine milieu supports de novo differentiation of IL-17-producing T cells. *Immunity* 24: 179–189.
8. Bettelli, E., Y. Carrier, W. Gao, T. Korn, T. B. Strom, M. Oukka, H. L. Weiner, and V. K. Kuchroo. 2006. Reciprocal developmental pathways for the generation of pathogenic effector TH17 and regulatory T cells. *Nature* 441: 235–238.
9. Mangan, P. R., L. E. Harrington, D. B. O'Quinn, W. S. Helms, D. C. Bullard, C. O. Elson, R. D. Hatton, S. M. Wahl, T. R. Schoeb, and C. T. Weaver. 2006. Transforming growth factor-β induces development of the T_H17 lineage. *Nature* 441: 231–234.
10. Weaver, C. T., L. E. Harrington, P. R. Mangan, M. Gavrieli, and K. M. Murphy. 2006. Th17: an effector CD4 T cell lineage with regulatory T cell ties. *Immunity* 24: 677–688.
11. Aggarwal, S., N. Ghilardi, M. H. Xie, F. J. de Sauvage, and A. L. Gurney. 2003. Interleukin-23 promotes a distinct CD4 T cell activation state characterized by the production of interleukin-17. *J. Biol. Chem.* 278: 1910–1914.
12. Zheng, Y., D. M. Danilenko, P. Valdez, I. Kasman, J. Eastham-Anderson, J. Wu, and W. Ouyang. 2007. Interleukin-22, a T_H17 cytokine, mediates IL-23-induced dermal inflammation and acanthosis. *Nature* 445: 648–651.
13. Begum, N. A., K. Ishii, M. Kurita-Taniguchi, M. Tanabe, M. Kobayashi, Y. Moriwaki, M. Matsumoto, Y. Fukumori, I. Azuma, K. Toyoshima, and T. Seya. 2004. *Mycobacterium bovis* BCG cell wall-specific differentially expressed genes identified by differential display and cDNA subtraction in human macrophages. *Infect. Immun.* 72: 937–948.
14. McKenzie, B. S., R. A. Kastelein, and D. J. Cua. 2006. Understanding the IL-23-IL-17 immune pathway. *Trends Immunol.* 27: 17–23.
15. Tsuji, S., M. Matsumoto, O. Takeuchi, S. Akira, I. Azuma, A. Hayashi, K. Toyoshima, and T. Seya. 2000. Maturation of human dendritic cells by cell wall skeleton of *Mycobacterium bovis* bacillus Calmette-Guérin: involvement of toll-like receptors. *Infect. Immun.* 68: 6883–6890.
16. Langowski, J. L., X. Zhang, L. Wu, J. D. Mattson, T. Chen, K. Smith, B. Basham, T. McClanahan, R. A. Kastelein, and M. Oft. 2006. IL-23 promotes tumour incidence and growth. *Nature* 442: 461–465.
17. Kryczek, I., S. Wei, L. Zou, S. Altuwaijri, W. Szeliga, J. Kolls, A. Chang, and W. Zou. 2007. Cutting edge: Th17 and regulatory T cell dynamics and the regulation by IL-2 in the tumor microenvironment. *J. Immunol.* 178: 6730–6733.
18. Kolls, J. K., and A. Linden. 2004. Interleukin-17 family members and inflammation. *Immunity* 21: 467–476.
19. Takahashi, H., M. Numasaki, M. T. Lotze, and H. Sasaki. 2005. Interleukin-17 enhances bFGF-, HGF- and VEGF-induced growth of vascular endothelial cells. *Immunol. Lett.* 98: 189–193.
20. Numasaki, M., J. Fukushi, M. Ono, S. K. Narula, P. J. Zavodny, T. Kudo, P. D. Robbins, H. Tahara, and M. T. Lotze. 2003. Interleukin-17 promotes angiogenesis and tumor growth. *Blood* 101: 2620–2627.
21. Matsumoto, M., T. Seya, S. Kikkawa, S. Tsuji, K. Shida, M. Nomura, M. Kurita-Taniguchi, H. Ohigashi, H. Yokouchi, K. Takami, et al. 2001. Interferon γ-producing ability in blood lymphocytes of patients with lung cancer through activation of the innate immune system by BCG cell wall skeleton. *Int. Immunopharmacol.* 1: 1559–1569.
22. Sakuma, T., K. Kodama, T. Hara, Y. Eshita, N. Shibata, M. Matsumoto, T. Seya, and Y. Mori. 1993. Levels of complement regulatory molecules in lung cancer: disappearance of the D17 epitope of CD55 in small-cell carcinoma. *Jpn. J. Cancer Res.* 84: 753–759.
23. Akazawa, T., H. Masuda, Y. Saeki, M. Matsumoto, K. Takeda, K. Tsujimura, K. Kuzushima, T. Takahashi, I. Azuma, S. Akira, et al. 2004. Adjuvant-mediated tumor regression and tumor-specific cytotoxic response are impaired in MyD88-deficient mice. *Cancer Res.* 64: 757–764.
24. Azuma, I., E. E. Ribi, T. J. Meyer, and B. Zbar. 1974. Biologically active components from mycobacterial cell walls: I. Isolation and composition of cell wall skeleton and component P3. *J. Natl. Cancer Inst.* 52: 95–101.
25. Barnden, M. J., J. Allison, W. R. Heath, and F. R. Carbone. 1998. Defective TCR expression in transgenic mice constructed using cDNA-based α- and β-chain genes under the control of heterologous regulatory elements. *Immunol. Cell Biol.* 76: 34–40.
26. Livak, K. J., and T. D. Schmittgen. 2001. Analysis of relative gene expression data using real-time quantitative PCR and the $2^{-\Delta CT}$ method. *Methods* 25: 402–408.

27. Wilson, M. C., V. N. Jackson, C. Heddle, N. T. Price, H. Pilegaard, C. Juel, A. Bonen, I. Montgomery, O. F. Hutter, and A. P. Halestrap. 1998. Lactic acid efflux from white skeletal muscle is catalyzed by the monocarboxylate transporter isoform MCT3. *J. Biol. Chem.* 273: 15920–15926.
28. Saio, M., S. Radoja, M. Marino, and A. B. Frey. 2001. Tumor-infiltrating macrophages induce apoptosis in activated $CD8^+$ T cells by a mechanism requiring cell contact and mediated by both the cell-associated form of TNF and nitric oxide. *J. Immunol.* 167: 5583–5593.
29. Kim, J. W., and C. V. Dang. 2006. Cancer's molecular sweet tooth and the Warburg effect. *Cancer Res.* 66: 8927–8930.
30. Gatenby, R. A., and R. J. Gillies. 2004. Why do cancers have high aerobic glycolysis? *Nat. Rev. Cancer* 4: 891–899.
31. Walenta, S., and W. F. Mueller-Klieser. 2004. Lactate: mirror and motor of tumor malignancy. *Semin. Radiat. Oncol.* 14: 267–274.
32. Heinemeyer, T., E. Wingender, I. Reuter, H. Hermjakob, A. E. Kel, O. V. Kel, E. V. Ignatieva, E. A. Ananko, O. A. Podkolodnaya, F. A. Kolpakov, et al. 1998. Databases on transcriptional regulation: TRANSFAC, TRRD, and COMPEL. *Nucleic Acids Res.* 26: 362–367.
33. Halestrap, A. P., and N. T. Price. 1999. The proton-linked monocarboxylate transporter (MCT) family: structure, function, and regulation. *Biochem. J.* 343: 281–299.
34. Trinchieri, G. 2003. Interleukin-12 and the regulation of innate resistance and adaptive immunity. *Nat. Rev. Immunol.* 3: 133–146.
35. Bronte, V., D. B. Chappell, E. Apolloni, A. Cabrelle, M. Wang, P. Hwu, and N. P. Restifo. 1999. Unopposed production of granulocyte-macrophage colony-stimulating factor by tumors inhibits $CD8^+$ T cell responses by dysregulating antigen-presenting cell maturation. *J. Immunol.* 162: 5728–5737.
36. Flo, T. H., O. Halaas, S. Torp, L. Ryan, E. Lien, B. Dybdahl, A. Sundan, and T. Espevik. 2001. Differential expression of Toll-like receptor 2 in human cells. *J. Leukocyte Biol.* 69: 474–481.
37. Gladden, L. B. 2004. Lactate metabolism: a new paradigm for the third millennium. *J. Physiol.* 558: 5–30.
38. Walenta, S., M. Wetterling, M. Lehrke, G. Schwickert, K. Sundfor, E. K. Rofstad, and W. Mueller-Klieser. 2000. High lactate levels predict likelihood of metastases, tumor recurrence, and restricted patient survival in human cervical cancers. *Cancer Res.* 60: 916–921.
39. Schwickert, G., S. Walenta, K. Sundfor, E. K. Rofstad, and W. Mueller-Klieser. 1995. Correlation of high lactate levels in human cervical cancer with incidence of metastasis. *Cancer Res.* 55: 4757–4759.
40. Walenta, S., A. Salameh, H. Lyng, J. F. Evensen, M. Mitze, E. K. Rofstad, and W. Mueller-Klieser. 1997. Correlation of high lactate levels in head and neck tumors with incidence of metastasis. *Am. J. Pathol.* 150: 409–415.
41. Fantin, V. R., J. St.-Pierre, and P. Leder. 2006. Attenuation of LDH-A expression uncovers a link between glycolysis, mitochondrial physiology, and tumor maintenance. *Cancer Cell* 9: 425–434.
42. Gottfried, E., L. A. Kunz-Schughart, S. Ebner, W. Mueller-Klieser, S. Hoves, R. Andreesen, A. Mackensen, and M. Kreutz. 2006. Tumor-derived lactic acid modulates dendritic cell activation and antigen expression. *Blood* 107: 2013–2021.
43. Fischer, K., P. Hoffmann, S. Voelkl, N. Meidenbauer, J. Ammer, M. Edinger, E. Gottfried, S. Schwarz, G. Rothe, S. Hoves, et al. 2007. Inhibitory effect of tumor cell-derived lactic acid on human T cells. *Blood* 109: 3812–3819.
44. Murray, C. M., R. Hutchinson, J. R. Bantick, G. P. Belfield, A. D. Benjamin, D. Brazma, R. V. Bundick, I. D. Cook, R. I. Craggs, S. Edwards, et al. 2005. Monocarboxylate transporter MCT1 is a target for immunosuppression. *Nat. Chem. Biol.* 1: 371–376.

Teleost TLR22 Recognizes RNA Duplex to Induce IFN and Protect Cells from Birnaviruses[1]

Aya Matsuo,[2]* Hiroyuki Oshiumi,[2]* Tadayuki Tsujita,[3]* Hiroshi Mitani,[†] Hisae Kasai,[‡] Mamoru Yoshimizu,[‡] Misako Matsumoto, and Tsukasa Seya[4]*

TLR22 occurs exclusively in aquatic animals and its role is unknown. Herein we show that the fugu (*Takifugu rubripes*) (fg)TLR3 and fgTLR22 link the IFN-inducing pathway via the fg Toll-IL-1R homology domain-containing adaptor protein 1(fgTICAM-1, or TRIF) adaptor in fish cells. fgTLR3 resides in endoplasmic reticulum and recognizes relatively short-sized dsRNA, whereas fgTLR22 recognizes long-sized dsRNA on the cell surface. On poly(I:C)-stimulated fish cells, both recruit fgTICAM-1, which in turn moves from the TLR to a cytoplasmic signalosome region. Thus, fgTICAM-1 acts as a shuttling platform for IFN signaling. When fish cells expressing fgTLR22 are exposed to dsRNA or aquatic dsRNA viruses, cells induce IFN responses to acquire resistance to virus infection. Thus, fish have a novel TICAM-1-coupling TLR that is distinct from the mammalian TLR3 in cellular localization, ligand selection, and tissue distribution. TLR22 may be a functional substitute of human cell-surface TLR3 and serve as a surveillant for infection with dsRNA virus to alert the immune system for antiviral protection in fish. ***The Journal of Immunology*, 2008, 181: 3474–3485.**

The type I IFN system is a host defense against microbial pathogens in animals (1, 2). In acute viral infections, IFN induces Mx and oligoadenylate synthetase to suppress viral replication (3). In late-phase infection it orchestrates cellular immunity including T and NK cells and protects hosts from persistent or repetitive viral infections (2, 4).

Earlier reports suggested that in mammalian fibroblasts, dsRNA (or its analog poly(I:C)) acts as an inducer for type I IFN, but the receptors for triggering IFN induction had not been identified until recently. Currently, in mammals, TLR3 on the endosomal membrane and retinoic acid-inducible gene I (RIG-I)[5] and melanoma differentiation-associated gene 5 (MDA5) in the cytoplasm are identified as sensors for dsRNA (1, 5). When viral genome RNA replicates in the cytoplasm, RIG-I and MDA5 sense it and assemble the adaptor mitochondrial antiviral signaling protein (MAVS; also called Cardif, IPS-1, orVISA) on the mitochondrial membrane (5). RIG-I preferentially recognizes 5′-phosphates of RNA (6, 7), whereas MDA5 recognizes the signature of dsRNA (8). They are distributed ubiquitously in cells/tissues and trigger IFN regulatory factor 3 (IRF-3) activation followed by type I IFN induction through the MAVS signal cascade (1, 2, 5). This intrinsic pathway appears to link main protective responses against RNA virus infection in mammals.

On the other hand, human TLR3 signals the presence of extrinsic dsRNA, recruits the adaptor Toll-IL-1R homology domain-containing adaptor protein 1 (TICAM-1), and induces IRF-3 activation followed by IFN-β promoter activation (1, 2, 9). Human TLR3 resides limitedly in myeloid dendritic cells, fibroblasts, and epithelial cells (10). TICAM-1 recruits TNF receptor-associated factor (TRAF) and TNF receptor-associated NF-κB kinase (TANK) family proteins for IFN-inducing signaling (11, 12; M. Sasai, H. Oshiumi, and T. Seya, unpublished data). NAK-associated protein 1 (NAP1), like other TANK family subunits (13), assembles two kinases, IKKε and TBK1, which activate the transcription factor IRF-3 (14). We call this extrinsic pathway the TICAM-1 pathway.

The TICAM-1 pathway and the cytoplasmic MAVS pathway converge on NAP1 to activate IRF-3 in human cells (15). Gene-disrupted mouse analyses show that TICAM-1 is involved in induction of the anti-mCMV immune response for host protection (16). The TICAM-1 pathway also appears to be involved in other DNA virus infections (16, 17). No clear involvement of TLR3 and TICAM-1 in defense against RNA virus infection has been offered using gene-disrupted mice, although many studies have anticipated that the TICAM-1 pathway has antiviral function against RNA viruses.

In fish studies, teleost IFN was recently discovered in the zebrafish (*Danio rerio*) (18), and since has been found in many fish species (19). Although the predicted protein sequence of the fish IFN has low

*Department of Microbiology and Immunology, Hokkaido University Graduate School of Medicine, Sapporo, Japan; †Department of Integrated Biosciences, University of Tokyo, Chiba, Japan; and ‡Faculty of Fisheries Sciences, Hokkaido University, Hakodate, Japan

Received for publication November 14, 2007. Accepted for publication June 20, 2008.

The costs of publication of this article were defrayed in part by the payment of page charges. This article must therefore be hereby marked *advertisement* in accordance with 18 U.S.C. Section 1734 solely to indicate this fact.

[1] This work was supported in part by CREST-JST (Japan Science and Technology Corporation), by Grants-in-Aid from the Ministry of Education, Science, and Culture (Specified Project for Advanced Research) and the Ministry of Health, Labor, and Welfare of Japan, and by the Takeda Science Foundation, Uehara Memorial Foundation, Northtec Foundation, Akiyama Foundation, and Mitsubishi Foundation. Financial support by the Sapporo Biocluster "Bio-S", the Knowledge Cluster Initiative of the MEXT, and the Program of Founding Research Centers for Emerging and Reemerging Infectious Diseases, MEXT, are gratefully acknowledged.

[2] A.Y. and H.O. contributed equally to this paper.

[3] Current address: Exploratory Research for Advanced Technology/Japan Science and Technology Center, Laboratory of Molecular and Developmental Biology, University of Tsukuba, Tennoudai 1-1-1, Tsukuba 305-8577, Japan.

[4] Address correspondence and reprint requests to Dr. Tsukasa Seya, Department of Microbiology and Immunology, Graduate School of Medicine, Hokkaido University, Kita-ku, Sapporo 060-8638, Japan. E-mail address: seya-tu@pop.med.hokudai.ac.jp

[5] Abbreviations used in this paper: RIG-I, retinoic acid-inducible gene I; BLAST, basic local alignment search tool; CPE, cytopathic effect; ER, endoplasmic reticulum; fg, *Takifugu rubripes*; HA, hemagglutinin; IPNV, infectious pancreatic necrosis virus; IRF-3, IFN regulatory factor 3; ISRE, IFN-stimulated regulatory element; LRR, leucine-rich repeat; MAVS, mitochondrial antiviral signaling protein; MDA5, melanoma differentiation-associated gene 5; moi, multiplicity of infection; NAP1, NAK-associated protein 1; PGN, peptidoglycan; rt, rainbow trout; polyC, polycytidylic acid; polyU, polyuridylic acid; $TCID_{50}$, 50% tissue culture-infective dose; TICAM-1, Toll-IL-1R homology domain-containing adaptor protein 1; TIR, Toll-IL-1 receptor; YFP, yellow fluorescent protein; zf, zebrafish.

(<20%) similarity to mammalian and avian type I IFNs, IFN-α and IFN-β, it up-regulates Mx and IFN-stimulated regulatory element (ISRE) promoter activation (18). Hence, fish possess IFN-inducing machinery. Since fish are exposed to viruses and RNA in water, they must have IFN-inducing receptors. However, no receptors for IFN induction have been identified yet in fish.

The existence of the TLR family in teleosts has been predicted from the genome database (20–23). According to the database of *Takifugu rubripes* (puffer fish), this teleost species possesses an ortholog of human TLR3 and other orthologs of human TLR members (20). Additionally, this teleost has a gene encoding a fish-specific TLR (hereafter called TLR22), whose functions are unknown. Fish may have a part of the gene of MDA5-like product, but its functional features are also unidentified. What happens in the IFN response during viral infection accordingly remains to be addressed in fish.

We found TLR22 in many aquatic vertebrate species (19, 20, 24), but not in birds and land animals (24). In this study, we demonstrate that TLR22 is a dsRNA-recognizing pattern receptor that recruits TICAM-1 to induce IFN and exerts a protective role in fish cells against dsRNA virus infection.

Materials and Methods

Accession numbers

Accession numbers for all genes used in this study are listed below: *T. rubripes* (fg)TLR22 (AB197916), rainbow trout (rt)TLR22-1 (AJ628348), rtTLR22-2 (AJ878915), rtTLR3 (DQ459470), rtIFN (AJ582754), and infectious pancreatic necrosis virus (IPNV) (NC001915). Rainbow trout has two orthologs of fgTLR22, rtTLR22-1 and rtTLR22-2, which were 93.0% homologous to each other (data not shown). Appropriate primers for detection of mRNAs of these genes are listed in Table I.

Cells and reagents

Human HEK293 or HeLa cells were cultured as described previously (10). A fibroblast-like cell line (OLHd-rRe3) of Japanese medaka fish, *Oryzias latipes*, was cultured in L-15 medium containing 20% heat-inactivated FCS and 10 mM HEPES at 33°C. RTG-2 cells derived from rainbow trout were cultured in a medium containing 10% heat-inactivated FCS and antibiotics (100 U/ml penicillin and 100 μg/ml streptomycin) at 20°C. LPS was purchased from BD Biosciences. Peptidoglycan (PGN) was purified from *Staphylococcus aureus* (Fluka). All nucleotide primers and oligodeoxynucleotides (ODN) containing CpG motifs (CpG-ODN) were purchased from Sigma-Genosys. Poly(I:C), polycytidylic acid (polyC), polyuridylic acid (polyU), and poly(dI:dC) were purchased from Amersham Biosciences. Variable-sized dsRNAs were transcribed from a cDNA template of measles virus with MEGAscript (Ambion) in vitro.

Molecular cloning of T. rubripes *DNAs*

First-strand cDNAs were reverse-transcribed from random-primed RNA templates extracted from *T. rubripes* kidney or eye tissues using M-MLV(−) reverse transcriptase (Promega). FgTLR3, fgTLR22, and fgTICAM-1 full-length cDNA fragments were amplified by PCR using primers shown in Table I. The PCR products were cloned using pCR-Blunt vector (Invitrogen). Several independent clones were subjected to DNA sequencing using ABI 3100 sequencer (PE Applied Biosystems) for assessing sequence accuracy. IFN of *T. rubripes* was searched by homology to zebrafish IFN using the basic local alignment search tool (BLAST) server. The 5′ promoter region identified from *T. rubripes* genomic DNA as −1 to −777 was subcloned into pEFBOS vector. FgMyD88 Toll-IL-1 receptor (TIR) domain was found in the *T. rubripes* database by BLAST search with reference to the human MyD88 protein sequence, and amplified by PCR using the primers shown in Table I.

cDNA expression vector

The cDNAs encoding fgTLR3 and fgTLR22 were placed between the *Xho*I and *Not*I sites of the pFEBOS expression vector. Flag-, hemagglutinin (HA)-, and Myc-tags were attached to the C- or N-terminus of the proteins as described previously (15, 25). Constitutively active CD4/TLR22 was constructed by fusing cDNAs encoding the extracellular domain of huCD4 (from 1 to 391 aa region) to the transmembrane and cytoplasmic domains of fgTLR22 (from 565 to 935 aa region). The obtained chimera CD4/TLR22 construct was placed between the *Xho*I and *Not*I sites of pEFBOS. Flag-tag was inserted just before the stop codon of fgTLR22 and placed between the *Xho*I and *Not*I sites of pEFBOS. To make the fgTLR22-myc expression vector, myc-tag was added to the C-terminal end of the signal peptide sequence of fgTLR22 and subcloned into *Xho*I and *Not*I sites of the pEFBOS expression vector. FgTLR3-yellow fluorscent protein (YFP) expression vector was constructed by inserting the full-length fgTLR3 into the pEYFP-N1 vector at the *Xho*I and *Kpn*I sites. The constructs of the dominant-negative human TICAM-1 (TICAM TIR (P434H)) and MyD88 (TIR) were described previously (25). Dominant-negative forms of fgTICAM-1 and fgMyD88 were constructed as human dominant-negative counterparts. Precisely, cDNA encoding the 341–479 aa region of fgTICAM was inserted into the pEFBOS *Xho*I-*Not*I sites and substituted proline at 382 with histidine. The fgMyD88 TIR domain-encoding region (152–288 aa region) was subcloned into the *Xho*I-*Not*I sites of pEF-BOS.

Table I. *Primer list*

Primer Name[a]	Sequence
fgTLR22-F	CTCAGAGCTTTGTGGTGTCT
fgTLR22-R	TTGCTTCTCTGATTAAGCCC
fgTLR3-F	CCAAGTGAAAACCACACGCA
fgTLR3-R	CTGGGACAACGGGACCTTT
fgTICAM-F	CATCTCTGCTGAATGGGG
fgTICAM-R	GTGGTGTAATGGACTGTAG
fgMyD88-F	CTCGGTAGGTCCAGTTTTC
fgMyD88-R	TCCTGCACCATATTCTGC
fgIFN promoter-F	TTGAATGGAAACAAGTCAGT
fgIFN promoter-R	CTTTCACTCAAGGAGGTCGC
rtIFN-F	CTGACCGGATGCAGAAGGA
rtIFN-R	TGGAGAGAGAAGCCAAGATGGA
rtTLR22-F	CTTTGATGAGCAGAAGGACG
rtTLR22-R	CTAAAGCCAGCCGTAGTTGC
rtβ-actin-F	CCTGTGTATCACCTGCCATGA
rtβ-actin-R	ACGCCTGTGCACTGTAGTTCA

[a] F indicates forward; R, reverse.

Reporter gene assay

HEK293 cells (1×10^6 cells/well) were transiently transfected in 24-well plates using Lipofectamine 2000 reagent (Invitrogen) with pEFBOS human TLR2, human TLR3, human TLR4, human TLR9, fgTLR3, fgTLR22 (200 ng), dominant-negative human TICAM-1 (P434H), human MyD88 (TIR) (50, 200 ng) or empty vector, together with a luciferase-linked IFN-β promoter gene (Stratagene, 100 ng). RTG-2 cells (1×10^6 cell/well) were transiently transfected in 24-well plates using FuGene HD (Roche) with fgTLR22, fgTLR3 (200 ng), dominant-negative fgTICAM-1 (50 or 200 ng), or empty vector together with a luciferase-linked fgIFN promoter gene. In some experiments, stable clones with this gene (named RTG (Luc-fgIFN) cells) were used instead of human IFN reporter. phRL-TK vector (1 ng) (Promega) was used as an internal control. Twenty-four hours after transfection, cells were stimulated with LPS (100 ng/ml), PGN (10 μg/ml), CpG (2 mM), or poly(I:C) (10 or 50 μg/ml), polyC (10 μg/ml), polyU (10 μg/ml), poly(dI:dC) (10 μg/ml), and in vitro-transcribed dsRNA (typically 10 μg/ml) for 6 h. The cells were lysed with lysis buffer (Promega) and luciferase activity was measured using a dual-luciferase reporter assay kit (Promega) with luminometer (Berthold Technologies). Specific activity was calculated from light intensity measurements with a *Renilla* luciferase internal control. Values were expressed as mean relative stimulation with SD from triplicate values from a minimum of three separate experiments.

Confocal microscopy

HeLa, OLHd-rRe3, and RTG-2 cells were plated onto coverglass in a 24-well plate. In the following day, cells were transfected with indicated plasmids using FuGene HD. The amount of DNA was kept constant by adding empty vector. After 24 h, cells were stimulated with poly(I:C) and fixed with 3% of formaldehyde in PBS as indicated periods, and then washed four times with PBS. Cells were permeabilized with PBS containing 0.2% Triton X-100 for 15 min. Permeabilized cells were blocked with PBS containing 1% BSA, and were labeled with anti-Flag mAb (Sigma-Aldrich) or anti-HA pAb (Sigma-Aldrich) in 1% BSA/PBS for 1 h at room temperature. The cells were then washed with 1% BSA/PBS and treated for 30 min at room temperature with Alexa-conjugated Abs (Molecular Probes). For

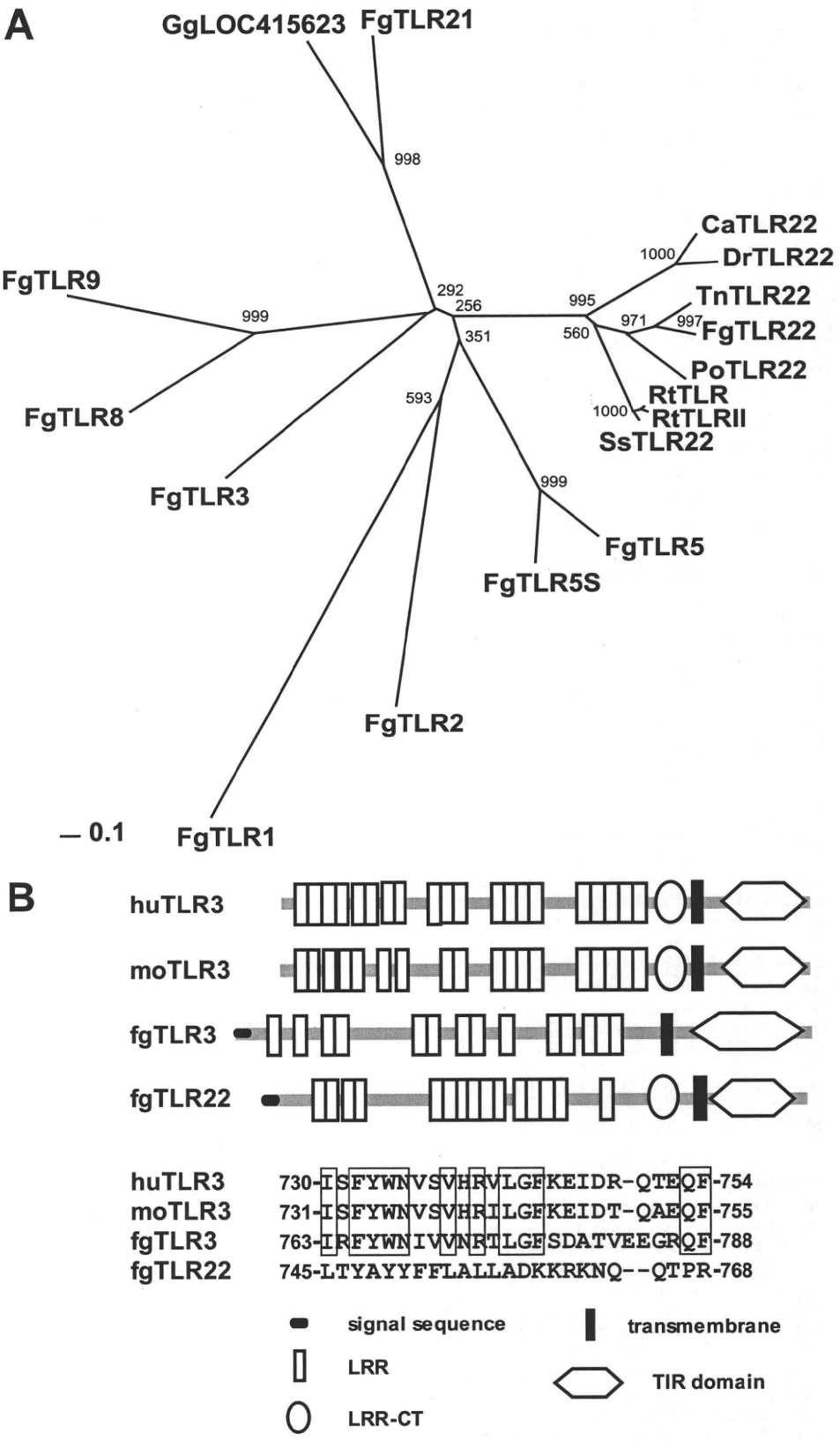

FIGURE 1. Structures and phylogenic analysis of TLR3 and TLR22. *A*, Gene tree for fgTLR22. Teleost and chicken TLR protein sequences were aligned with ClustalW on DDBJ server, and the phylogenic tree was made by a neighbor-joining method program. Number on each node represents bootstrap probability that is 1000× reiteration. Fg, Ca, Dr, Tn, Po, Rt, and Ss stand for *Takifugu rubripes*, *Carassius auratus*, *Danio rerio*, *Tetradon nigroviridis*, *Paralichthys olivaceus*, rainbow trout, or *Salmo salar*. GgLOC415623 is a chicken protein that is most similar to fgTLR22. The protein was classified into TLR21 by the phylogenic tree. *B*, Motif structures of human, mouse, and fugu TLR3 and fugu TLR22. Possible domain structures of the fish TLRs were obtained with SMART search according to the primary sequences. Vertical open bars represent LRRs and filled bars represent transmembrane domains. LRR-CT (the leucine-rich repeat at the C terminus) is shown by circles. The signal sequences are shown to the left and TIRs are to the right. Amino acid sequence alignment of the linker regions of huTLR3, moTLR3, fgTLR3, and fgTLR22 are shown at the bottom.

organelle marker staining, cells were treated with calnexin (StressGen Biotechnologies) and then FITC-labeled goat anti-mouse IgG secondary Ab. In some cases cells were prestained with anti-TLR Abs. Thereafter, microcoverglasses were mounted onto a slide glass using PBS containing 2.3% 1,4-diazabicyclo(2.2.2)octane (DABCO) and 50% of glycerol. In some experiments, we used YFP-labeled fgTLR3 instead of tagged fgTLR3, since the background by the secondary Ab (against tag) was increased for unknown reasons in the case of fgTLR3. The stained cells were visualized at ×60 magnification under a FluoView (Olympus).

Isolation of IPNV RNA

IPNV was propagated with RTG-2 cells. RTG-2 cells cultured in a 75-cm^2 T flask were infected with IPNV. After 4–7 days incubation, viruses were

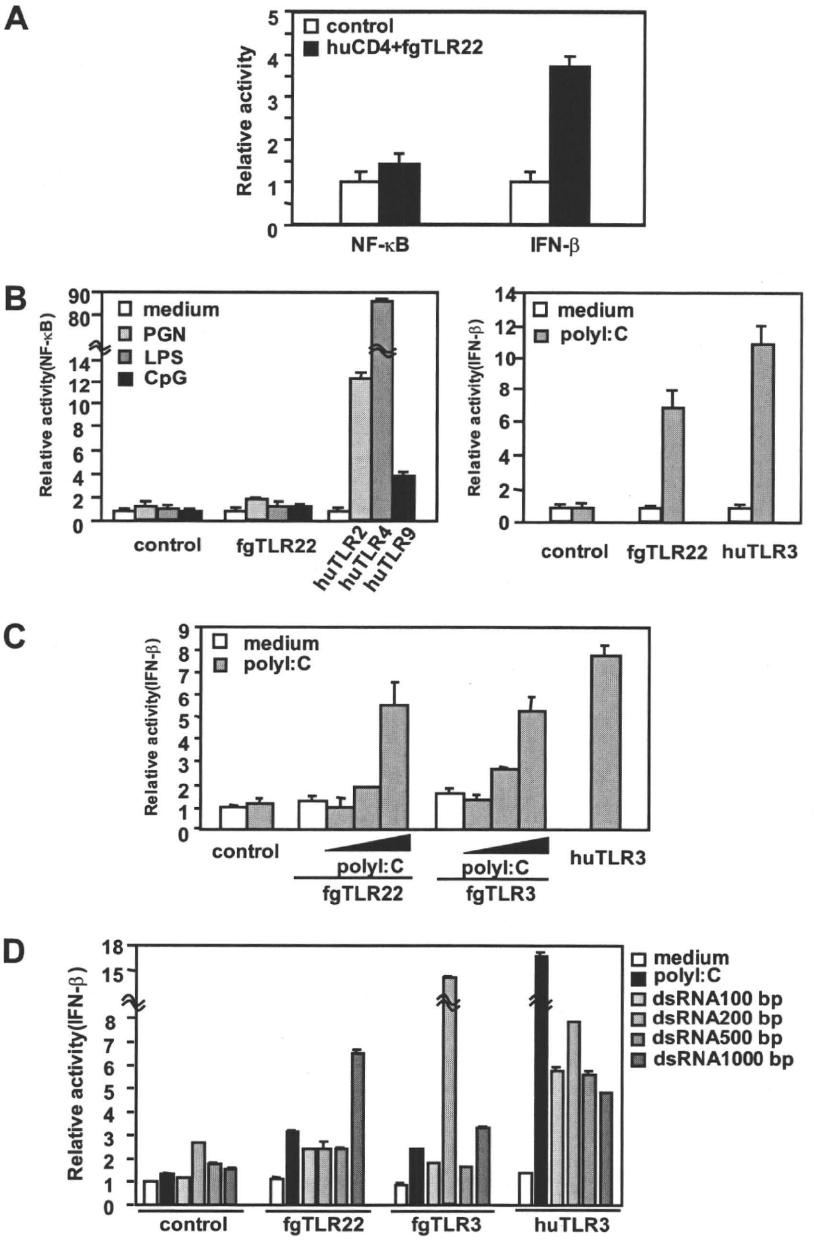

FIGURE 2. Human cells expressing fgTLR22 induce activation of the human IFN-β promoter in response to poly(I:C). *A*, HEK293 cells were transfected with expression vector for CD4 + TLR22, where the cytosolic domain of fgTLR22 (the TIR domain) was fused to the extracellular portion of CD4. The amount of DNA transfected was equalized with empty expression vector, which was also used as the control. Reporter activity was determined as described in the text. *B*, HEK293 cells were transfected with fgTLR22 (full-length)-expressing vector or pEFBOS (vector only). Twenty-four hours after transfection, cells were stimulated with PGN (10 μg/ml), LPS (100 ng/ml), and CpG (2 μM) for 6 h and NF-κB promoter activation was determined (*left panel*). *Right panel*, poly(I:C) (50 μg/ml) was used instead of other stimulators, and relative IFN-β promoter activation by poly(I:C) was compared between fgTLR22 and human (hu)TLR3. *C*, HEK cells were transfected with the vector for expression of huTLR3, fgTLR22, or fgTLR3. pEFBOS and pEFBOS (huTLR3) were used as controls. Twenty-four hours after transfection, cells were stimulated with poly(I:C) (5, 10, 50 μg/ml) for 6 h. IFN-β promoter activation was measured by luciferase activity in the cell lysates. *D*, Cells were transfected with full-length fgTLR22- or fgTLR3-expressing vector. pEFBOS was a control for vector only. Twenty-four hours later, cells were stimulated with 10 μg/ml of poly(I:C) or variable-sized (100-, 200-, 500-, and 1000-bp) dsRNA for 6 h. IFN-β promoter activation was measured by luciferase assay as in *C*.

harvested from infected cell lysates by freeze-thaw cycles. Cell debris was removed by centrifugation at 10 krpm for 10 min, and then virus particles were concentrated by ultracentrifuge at 23 krpm for 1 h. Viral RNA was extracted from 15 ml of these lysates with 500 μl of TRIzol (Invitrogen) according to the manufacturer's instructions.

Quantitative PCR

Total RNA of RTG-2 cells were extracted using TRIzol reagents, and cDNA was made by using MV-reverse transcriptase with random primers. iQ SYBER Green Supermix was used for PCR reactions and analyzed with iCycler iQ real-time PCR analyzing system (Bio-Rad). Primers for quantitative PCR are shown in Table I. Relative rtIFN mRNA levels were calculated by dividing the relative amounts of mRNA of rtIFN by those of the rainbow trout β-actin mRNA.

Immunoprecipitation

HEK293FT cells were transiently transfected with expression vectors in a 6-well plate using Lipofectamine 2000 reagent (Invitrogen) and incubated for 24 h. Cells were lysed with lysis buffer (25 mM Tris-HCl (pH 7.5), 150 mM NaCl, 1% of Nonidet P-40, 2 mM PMSF, 25 mM iodoacetaminde, 10 mM EDTA), and proteins were immunoprecipitated with anti-Flag mAb and then washed four times with lysis buffer. Obtained samples were analyzed by SDS-PAGE (7.5 or 10% gel) and Western blotting using anti-HA pAb (Sigma-Aldrich).

Titration of virus

RTG-2 cells (1×10^6 cells/well) were infected with IPNV (typical multiplicity of infection (moi) of 0.1). After 24 h, supernatants were serially 10-fold diluted and incubated with RTG-2 cells placed on a flat 96-well plate, and 100 μl medium with 8$\times$ dilution cycles was added to determine the 50% tissue culture-infective dose ($TCID_{50}$). Cells were incubated at 15°C for 7 days. On day 7 of incubation, the plates were examined for the presence of viral cytopathic effect (CPE) under the microscope.

Results

Identification of TLR22 in T. rubripes

We used the predicted protein sequence of fgTLR22 for a BLASTP search on the National Center for Biotechnology Information (NCBI) BLAST server for a nonredundant database, and found that teleosts and frogs (*Xenopus tropicalis*) have TLR22 orthologs by phylogenetic analyses (20, 24) (Fig. 1*A*). However, no expressed sequence tag or genome region encoding TLR22 was

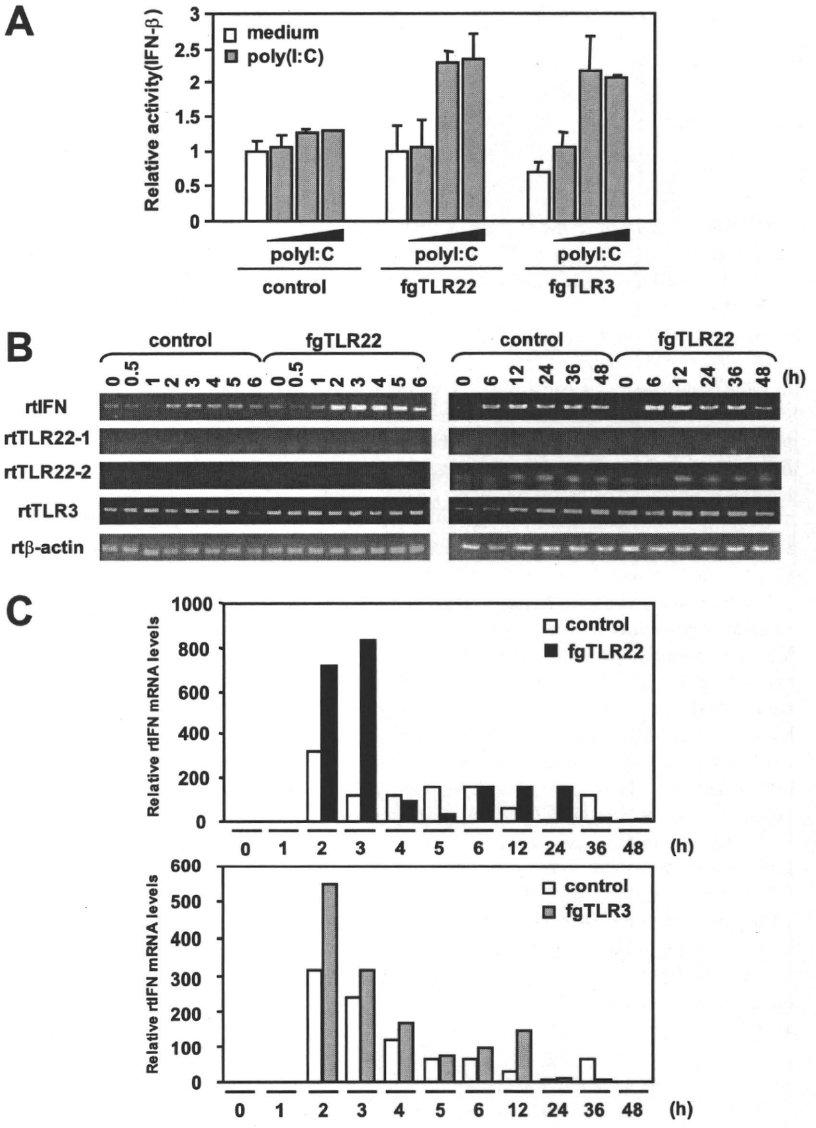

FIGURE 3. fgTLR22 recognizes poly(I:C) to induce fish IFN in fish cells. *A*, Rainbow trout RTG-2 cells were stably transfected with Luc-fgIFN vector (see *Materials and Methods*). The RTG (Luc-fgIFN) cells were then transiently transfected with fgTLR22 or fgTLR3 expression vector or control pEFBOS. Twenty-four hours later, cells were stimulated with poly(I:C) (5, 10, 50 μg/ml) for 6 h, and fgIFN promoter activation was determined by luciferase activity in the cell lysate. *B*, RTG-2 cells were transiently transfected with fgTLR22-expressing vector or control pEFBOS. Twenty-four hours later, cells were stimulated with poly(I:C) (25 μg/ml) for the indicated intervals. Since the rainbow trout possesses two mRNAs of TLR22, we referred them to rtTLR22–1 and rtTLR22–2. The mRNA levels of rtIFN, rtTLR22–1, rtTLR22–2, rtTLR3, and rtTICAM-1 were monitored by RT-PCR. The rtTICAM-1 message was constitutively expressed irrespective of poly(I:C) stimulation (data not shown). rtβ-actin was used for the control. PCR products were analyzed by gel electrophoresis (1.5% TAE agarose) and visualized with ethidium bromide (1 μg/ml). Three individual experiments were performed, and a representative one is shown. *C*, RTG-2 cells were transfected with pEFBOS (fgTLR22), pEFBOS (fgTLR3), or empty pEFBOS. Twenty-four hours later, cells were stimulated with poly(I:C) (25 μg/ml) for the indicated periods. The mRNA levels of rtIFN were measured by quantitative PCR. Relative fold induction against rtβ-actin level is shown. The experiments were performed three times and representative results are shown.

found in mammals and birds. Thus, these homology search analyses indicate that the TLR22 gene is conserved across aquatic vertebrates. To further confirm the absence of the TLR22 gene in the chicken genome, we conducted a TBLASTN search with fgTLR22 against the *Gallus gallus* whole genome. The best hits sequence in the chicken genome was the region encoding LOC415623, but the protein was an ortholog of TLR21 (data not shown). In the mouse genome, the most similar sequence to fgTLR22 was mouse TLR13. These analyses confirmed that TLR22 is conserved in vertebrates living in water or wet conditions, but not in animals living on land.

We cloned the fgTLR22 cDNA from the kidney and eye of *T. rubripes* to test its function. The cDNA sequence of the isolated fgTLR22 was identical to the sequence we previously predicted, and its open reading frame was encoded by three exons (20). The fgTLR22 protein had 15 leucine-rich repeats (LRRs) and one C-terminal LRR domain at the extracellular region and a TIR domain in the cytoplasmic region, suggesting that fgTLR22 possesses a typical structure of TLR but differs in the primary structure from TLR3 (Fig. 1*B*).

IFN promoter activation by fgTLR22 in a human cell line

Vertebrate IFN promoter and NF-κB activation has been determined successfully using human cells that have the human TLR signal system (26, 27). Thus, we first tested the functional ability of the TIR domain of fgTLR22 in human cell line HEK293. To estimate the output of fgTLR22 signaling, we made a chimera protein in which the Ig-like domain of CD4 was ligated with the transmembrane and intracellular region of fgTLR22. The human TLR4-CD4 chimera construct is known to activate the downstream signal of TLR4 by dimerization of the extracellular CD4 region (28). We examined whether the CD4-fgTLR22 chimera protein activates the human IFN-β promoter or NF-κB. The chimera protein was coexpressed in human HEK293 cells with an IFN-β promoter or NF-κB reporter plasmid. We observed minimal activation of NF-κB and about a 4-fold significant activation of the IFN-β promoter by expression of the chimera protein (Fig. 2*A*), suggesting that the TIR domain of fgTLR22 retains the capacity to activate the human IFN-β promoter and, to a lesser extent, the transcription factor NF-κB in human cells.

Ligand properties of fgTLR22 in comparison with those of fgTLR3

The functional ability of fgTLR22 in HEK293 cells encouraged us to look for the ligand of fgTLR22. We subcloned the fgTLR22 full-length cDNA into the expression vector pEFBOS and transfected it into human HEK293 cells with reporter plasmids. FgTLR22 or mock-transfected cells were stimulated with PGN,

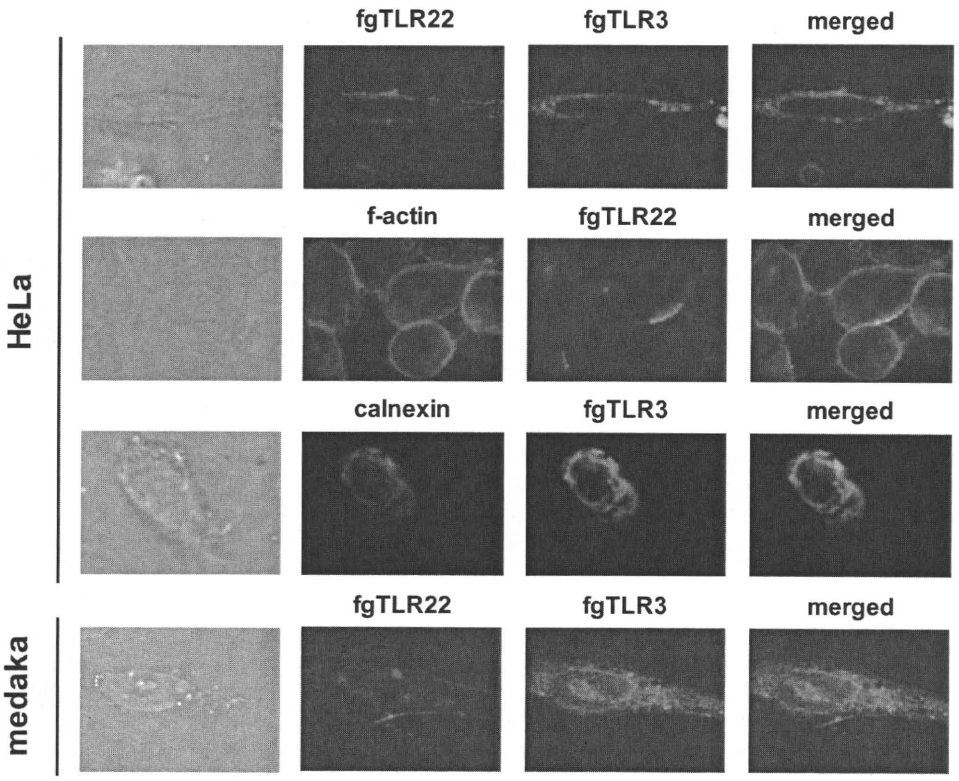

FIGURE 4. Localization of fgTLR22 and fgTLR3 in mammalian and fish cells. Confocal analysis using HeLa or medaka cells (OLHd-rRe3). fgTLR22 with C-terminal Flag, fgTLR3 with C-terminal YFP (green), and/or other markers were expressed in the indicated cells. fgTLR22 was labeled with mouse anti-Flag mAb and stained with Alexa 568-conjugated (red) or Alexa 488-conjugated (green, only in the second column) goat anti-mouse IgG. Cells were then treated with mAbs against Calnexin (ER marker) or f-actin (cytoskeleton marker) and Alexa 568-conjugated goat anti-mouse IgG. Phase-contrast features of cells are shown to the left. Cells were analyzed on FluoView.

LPS, CpG, or poly(I:C) for 6 h, and cell lysates were then prepared to measure reporter activation. PGN, LPS, and CpG activated neither NF-κB nor the IFN-β promoter via fgTLR22, although they activated the reporter via stimulation of the relevant human TLRs. In contrast, only poly(I:C) significantly activated the IFN-β promoter in fgTLR22-expressing cells (Fig. 2*B*). Thus, poly(I:C) is a ligand for fgTLR22. Because *T. rubripes* possesses an ortholog of TLR3 (20), we cloned fgTLR3 and measured the IFN-β promoter activation induced by poly(I:C) in fgTLR3-expressing cells. fgTLR3 also conferred the responsiveness to poly(I:C) on HEK293 cells in a way similar to fgTLR22 (Fig. 2*C*). Hence, the *T. rubripes* possesses two types of TLRs that recognize poly(I:C).

We next compared the response of fgTLR3 and fgTLR22 to polyU, polyC, poly(dI:dC), poly(I:C), and dsRNA using HEK transfectants. Ultimately, poly(I:C) and in vitro-transcribed dsRNA, but not polyU, polyC, or poly(dI:dC), activated the reporter in fgTLR22- or fgTLR3-expressing cells (data not shown), suggesting that both fgTLR22 and TLR3 signal the presence of dsRNA in human cells.

Next, we used various sizes of in vitro-transcribed dsRNA (29). Human TLR3 activated reporter genes in response to variable-sized dsRNA to similar extents irrespective of the length of dsRNA. In contrast, fgTLR22 and fgTLR3 showed different properties on responsiveness to variable-sized dsRNAs. In fgTLR22-expressing cells, 1000-bp dsRNA most strongly activated the reporter gene, but in fgTLR3-expressing cells, 200-bp dsRNA induced preferential activation of the reporter (Fig. 2*D*). Therefore, fgTLR3, fgTLR22, and human TLR3 exhibit differences in preference to the size of dsRNA, although the three TLRs essentially confer response to poly(I:C) or dsRNA on HEK293 cells. These observations using the human cell indicate a unique role of fgTLR22 in poly(I:C) or dsRNA recognition.

IFN induction by fgTLR22 in fish cells

We assessed the function of fgTLR22 in a teleost fibroblastic cell line, RTG-2. Teleosts also have an ortholog of human IFN, but previous phylogenetic analyses suggest that fish IFN forms a clade distinct from that of mammalian type I IFNs (18). The zebrafish (zf) IFN can be induced by overexpression of zfTICAM-1 (30), and it exerts antiviral effects through the induction of antiviral protein like Mx (31). We cloned the promoter region of the *T. rubripes* IFN gene that corresponds to the zfIFN and fused it to the luciferase open reading frame. fgTLR22 is widely expressed in various tissues and cell lines (20). Of the cell lines tested, the rainbow trout cell line, RTG-2, expressed only minute levels of the rtTLR22/rtTLR3 messages, which allowed us to employ RTG-2 for the fgTLR3/22 reporter analyses.

The RTG-2 cells were transfectable, but the transfection efficacy was ~10% by lipofection. fgTLR22 protein showed 80.8% similarity to rtTLR22 (rtTLR22-1 and rtTLR22-2), which was barely expressed in both unstimulated and poly(I:C)-stimulated cells (see Fig. 3*B*). The TIR sequences of fgTLR22 and rtTLR22 were 93.8% similar (data not shown), suggesting that they are functionally compatible. We transfected fgTLR22, fgTLR3, or mock expression vectors into RTG-2 cells together with the fgIFN promoter reporter plasmid (Fig. 3*A*). At 24 h after transfection, cells were stimulated with poly(I:C). Cell lysate was prepared 6 h after poly(I:C) stimulation, and luciferase activities were measured. Poly(I:C) barely activated the fgIFN reporter in control cells, but significantly activated it in fgTLR22- or fgTLR3-transfected cells (Fig. 3*A*), as observed in the human reporter assay system.

We next examined whether fgTLR22 transmits the signal to the endogenous IFN promoter (Fig. 3*B*). The NCBI DNA database has two cDNA sequences of the IFN gene in rainbow trout (AJ582754 and AM235738). We examined the poly(I:C)-inducible IFN (AJ582754) expression through fgTLR22 stimulation with poly(I:C) by RT-PCR analysis. RTG-2 cells transfected with fgTLR22 or empty vectors were incubated with medium containing poly(I:C), and expression of rtIFN was examined by RT-PCR and quantitative PCR. The IFN mRNA expression was more strongly increased 2 h after poly(I:C) stimulation in fgTLR22-expressing cells